

Stochastic Simulators: An Overview with Opportunities

Evan Baker^{*} Pierre Barbillon[†] Arindam Fadikar[‡]
 Robert B. Gramacy[§] Radu Herbei[¶] David Higdon[§]
 Jiangeng Huang^{||} Leah R. Johnson[§] Anirban Mondal^{**}
 Bianica Pires^{††} Jerome Sacks^{‡‡} Vadim Sokolov^{§§}

Abstract

In modern science, deterministic computer models are often used to understand complex phenomena, and a thriving statistical community has grown around effectively analysing them. This review aims to bring a spotlight to the growing prevalence of stochastic computer models — providing a catalogue of statistical methods for practitioners, an introductory view for statisticians (whether familiar with deterministic computer models or not), and an emphasis on open questions of relevance to practitioners and statisticians. Gaussian process surrogate models take center stage in this review, and these, along with several extensions needed for stochastic settings, are explained. The basic issues of designing a stochastic computer experiment and calibrating a stochastic computer model are prominent in the discussion. Instructive examples, with data and code, are used to describe the implementation and results of various methods.

Keywords: Computer Model; Gaussian Process; Uncertainty Quantification; Emulator; Computer Experiment; Agent Based Model; Surrogates; Calibration

^{*}Primary and corresponding author: Department of Mathematics, University of Exeter; e.baker@exeter.ac.uk

[†]UMR MIA-Paris, AgroParisTech, INRA, Université Paris-Saclay, 75005, Paris, France

[‡]Argonne National Laboratory

[§]Department of Statistics, Virginia Tech

[¶]Department of Statistics, The Ohio State University

^{||}Department of Statistics, University of California, Santa Cruz

^{**}Department of Mathematics, Applied Mathematics, and Statistics, Case Western Reserve University

^{††}The MITRE Corporation

^{‡‡}National Institute of Statistical Sciences

^{§§}Systems Engineering and Operations Research, George Mason University

1 Introduction

Computer models, also known as simulators, are in use everywhere. These are programs which describe and approximate a process of interest, and typically require a set of inputs before providing some output. Deterministic simulators — running the code with the same inputs always produces the same output — are widely used in physical and engineering science. Statistics (Sacks et al., 1989; Kennedy and O’Hagan, 2001) and Applied Mathematics (Sullivan, 2015) play prominent roles in the design and analysis of experiments with these simulators and their use. Stochastic simulators — running the code with the same inputs can produce different output due to the presence of random elements — are also widely used. For example, agent-based models (ABMs), prevalent in social sciences, are designed to explore complex social phenomena. Similarly, epidemiological models aim to understand the course of a serious disease through a population. A major concern in the statistical study of deterministic simulators is coping with scarce data: incredibly complicated simulators may not support many runs even on high performance computers. In contrast, the randomness in stochastic simulators all but necessitates many runs to enable any adequate analysis, affecting the scale of complexity such simulators can bear. In addition, the prospect of replicate runs in stochastic simulators, introduces questions of balancing replication and exploration. This article examines such basic issues, identifies accessible and effective methods, and points to unresolved questions that should be addressed.

The following is a basic model of a stochastic simulator experiment. If the code is run at a (vector) input x producing a (scalar) output $y(x)$, this could be represented as:

$$y(x) = M(x) + v, \quad v \sim N(0, \sigma_v^2(x)), \quad (1.1)$$

where $M(x)$ is the expected value, $E[y(x)]$, of the output. The variability v accounts for the randomness of the stochastic simulator (caused by random number generation within the code). Its variance, σ_v^2 , often depends on x (the case of constant variance is subsumed). For deterministic simulators, $\sigma_v^2 = 0$.

Equation 1.1 is often used to model physical experiments, where the observation $y(x)$ is the result of a response function $M(x)$ plus measurement error or, for an observational study, where $M(x)$ is fit to the observations with residual variance. Though structurally the same, the capability of running the stochastic simulator at designed inputs (unlike observational studies) and of treating complex phenomena that cannot be feasibly treated via physical experiments, are major distinctions. Moreover, the v -term denotes *intrinsic* variability rather than measurement or residual error. As a result, the formulation of problems, the application of methods, and interpretation of results can differ from those stemming from the more traditional settings.

The choice of method, with its assumptions and limitations, is crucial for any analysis of an experiment. An inclination for simplicity and availability of software would encourage the use of a standard statistical regression model (for example, linear regression) for M with a constant σ_v^2 . That this approach is effective under some

circumstances, especially when the space of possible inputs X is small, begs the question of how reliable it can be as a general prescription. Complex systems modeled by a simulator may neither suggest nor allow much simplification. The methods described in this review allow the simulated data to guide the choice of method under general conditions with little, or no simplification.

1.1 Goals

We have three primary goals; all three relate to the cross-disciplinary nature of this topic.

One goal is to bring effective statistical methods to the attention of subject scientists and enable a deeper understanding of stochastic simulators in use. The descriptions of statistical tools used or cited below try to avoid getting bogged down in mathematical intricacies. Some details of individual methods are included to help in understanding the strengths and weaknesses of the methods. Application of a number of methods is exemplified on testbed cases (Section 2), and available software for methods are identified where possible.

A second goal is to familiarize statisticians with an area of major importance that is crucial to the formation of evidence-based policy. Statisticians are sorely needed in the study and application of agent-based models (ABMs) and stochastic simulators in general. Researchers familiar with deterministic simulation techniques will see immediate opportunities, but statistical expertise of all kinds is essential to advancing the study of stochastic simulators.

The analysis of stochastic simulators is a developing field with many problems remaining unsolved. The challenges are often driven by the scale of the problems and present a range of issues whose resolution requires close cooperation between statisticians, subject scientists, and computer scientists. A third goal of this paper is to spur that process.

The review is structured as follows: Section 3 describes the models that form the basis for the analyses; Section 4 is devoted to the often crucial question of what simulator runs to make. Section 5 addresses a common objective of simulation experiments: calibration. Section 6 discusses other models and objectives that, while important, have seen less statistical research attention. Finally, Section 7 summarizes conclusions and poses unanswered questions. The references here surely do not cover the entire body of work on stochastic simulators but, together with this overview, should provide adequate coverage of the particular problems discussed.

2 Example Simulators

A few specific stochastic simulators will be discussed throughout this review to aid understanding. The first serves as a motivating real world example. Two others, with deliberately tamped down complexity, are used in order to exhibit key features of the

methods presented in later sections. In some cases simpler strategies could be equally effective because the complexity of the problem has been greatly reduced. Since the data used are available, others can compare different strategies, but the demonstration purpose is the one that is relevant in the discussion and reported computations below.

2.1 The Ebola Epidemic of 2014

As an example of the complexities in stochastic simulators and how statistical methods can be essential in analysis of said simulators, we highlight the study conducted by Fadikar et al. (2018). In response to the Ebola epidemic of 2014, increased efforts in modeling infectious epidemics were spurred by the 2015 Ebola challenge problem (<https://www.ebola-challenge.org/>). A synthetic population representing the individuals in Liberia (population ~ 4.5 million) and their activity schedules, inducing a time-varying contact network of individuals and locations, was developed (see Adigaa et al., 2015, for details on how). An agent-based model for a given population was also developed (Bisset et al., 2009). Together, this ABM makes it possible to model a contagion spreading from one individual to another in Liberia. Equation 1.1 may appear to be overly simplistic for dealing with the time evolution of the Ebola output but that is addressed in Section 3.4.

The ABM is stochastic since the parameter for contagion, transmissibility, only controls the *probability* of infection given that an interaction occurs for a specified duration. The model is updated daily, with the progress of the disease determined by the activity schedule, contact details, and other epidemiological characteristics, some of them, such as transmissibility, having unknown values. Determining good input values for unknowns (*calibration*) is key to establishing a capability of *predicting* the duration of the epidemic from early data.

The complexity of this problem is clearly high. The solution by Fadikar et al. (2018) uses methods and ideas discussed in Sections 3.3.1 and 3.4 as well as Section 5 where results of that study are also described. While the scale of this simulator is too great to use for simple demonstration of methods described in this review, the applicability of those methods in the study of the Ebola epidemic serves here as evidence of their importance.

2.2 Fish Capture-Recapture

The second stochastic simulator we consider mimics the movements and schooling behavior of fish in a mark-recapture application. Mark and recapture involves capturing a sample of the population, marking and releasing them, and following up by capturing another sample and counting how many are marked – the recaptured. The number in the second round that are marked allows one to estimate for the total population (Begon et al., 1979). Rather than treat both the initial marking and subsequent recapture of fish as simple random samples from the population, the entire process can instead be modeled. A population of fish are initialized at random locations in a 2-d, rectangular

lake with boundary conditions. The fish begin moving and schooling according to simple, agent-based rules. After an initial period of time, 100 fish are marked as they pass through a “net” in this lake. After an additional period of time, 100 fish are captured using this same net. The number of previously marked fish in this “recapture” are recorded.

This agent-based model is a modified version of the flocking model developed in NetLogo, a multi-agent simulation environment (Wilensky, 1999). The collective behavior that emerges in the flocking model is the result of providing each individual agent with the same set of simple rules (Reynolds, 1987). The flocking model is modified to include the mark-recapture dynamics described above. This model can then be used to estimate the total size of a fish population, given a count of recaptured fish (see Section 5.3).

For this highly stylized model the only input considered is the number of fish in the total population and the output is the number of recaptured fish. Other inputs for this model control the individual movement rules of the fish. For simplicity these will be ignored here, making the Fish model a single-input (population size), single-output (number marked in recapture) simulator.

Given an observed, real world, number of recaptured fish; this simulator, or one like it, can be used to estimate the total size of a fish population (see Section 5.3 for an example), say for conservation reasons.

Code, and compiled Rmarkdown documents, corresponding to our analysis of this simulator can be found at <https://github.com/jhuang672/fish>. Running the simulator afresh will require the installation of NetLogo <https://ccl.northwestern.edu/netlogo/>.

2.3 Ocean Circulation

The third example is a stochastic simulator that models the concentration of oxygen in a thin water layer (around 2000m deep) in the South Atlantic ocean (McKeague et al., 2005; Herbei and Berliner, 2014). The physical model is described via an advection-diffusion equation (equation (4) of McKeague et al. (2005)), i.e., a non-linear partial differential equation (PDE) describing the dynamics of oxygen concentration in terms of the water velocities and diffusion coefficients. The example is simplified by taking the oxygen concentration to depend only on four inputs: two unknown diffusion constants, K_x and K_y , and the two site variables, latitude and longitude; all other inputs are held fixed at nominal values.

For a given set of inputs the solution of the advection-diffusion equation is not available in closed form. However, using theoretical results (Feynman, 1948; Kac, 1949), the solution can be closely approximated through an associated random process (Herbei and Berliner, 2014). With the given inputs, generating random paths of the process produces outcomes that approximate the solution to the PDE. Such stochastic approximations are numerous in physical sciences, either due to computational limitations, a lack of complete understanding of the underlying system, or because the system under

study is itself believed to be random.

Code, and compiled Rmarkdown documents, corresponding to our analysis of this simulator can be found at <https://github.com/Demiperimetre/Ocean>.

3 Statistical Models

An experiment of running a simulator and producing data whose output is described by Equation 1.1 can have a multitude of goals. A principal objective, and the one we focus on here, is using the simulated data to predict values of the simulator, and estimate the mean $M(x)$ and intrinsic variance $\sigma_v^2(x)$ at untried x s in a context where getting new runs of the simulator is not cost-free. When M is believed to be “simple” (for example, a polynomial function of the coordinates of x) there are many standard “classical” techniques that can be used to approximate M . For example, linear regression models and generalised linear models have been used by Andrianakis et al. (2017) and Marrel et al. (2012). Complex problems such as those in Sections 2.1 and 2.3 are less easily managed: specifying a functional form for complex M requires sufficient prior knowledge or a huge abundance of data, both of which are often lacking. A prime emphasis of this article is on methods that have been developed to cope with such concerns; adequate references for a variety of standard methods are available for simpler circumstances.

There are a range of factors that need to be taken into account before choosing a statistical model (hereon referred to as a surrogate model, as it acts as a surrogate for the computer model). In addition to methodological assumptions, it is important to consider the “context”, that is, the conditions of the particular problem being studied, leading to Equation 1.1 and its extensions. Some important contexts include:

- The space of inputs is usually a hyper-rectangle: each coordinate of an input x is constrained by upper and lower bounds. Though the relevant part of the Atlantic Ocean is not rectangular, Section 2.3 simplifies issues by taking a rectangular input space.
- The output y in Equation 1.1 is one-dimensional but multivariate output, often a function of time, is common.
- Some inputs may be categorical rather than numerical.
- The probability distribution of v , the variability, is often taken to be normal, but this is often invalid, as discussed in Section 2.1.

Stretching back to Sacks et al. (1989), a vast literature, mostly on deterministic simulators, has found that a Gaussian Process (GP) model produces a flexible, effective surrogate for M . This approach, and its modifications needed to address the presence of input dependent $\sigma_v^2(x)$ in Equation 1.1, can be effective for stochastic simulation as has been documented in the literature (e.g. Kleijnen, 2009, 2017) and will be apparent

below. A thorough intuitive explanation (for deterministic computer models) can be found in O’Hagan (2006). More technical descriptions of GPs from a statistical perspective can be found in Santner et al. (2018) and, from a machine learning perspective, in Rasmussen and Williams (2006). In brief, the use of GPs allows computer model runs to play the key role in selecting an appropriate surrogate and thereby enabling assessments of uncertainty.

3.1 Gaussian Process Surrogates

Assume that: the input space, X , is a hyper-rectangle in d -dimensions; the output, $y(x)$, is univariate (scalar); and that the variability is normally distributed. In addition, assume:

- A1 The variability, v , has constant variance σ_v^2
- A2 The mean $M(x) = \mu + Z(x)$
- A3 μ is constant
- A4 $Z(\cdot)$ is a Gaussian Process on X with mean 0 and covariance function K , deconstructed as a product of a variance σ_Z^2 and a correlation function C .

The technical definition of a GP (Assumption A4) is: for *any* finite N and collection of inputs $X_N = (x_1, \dots, x_N)$, $Z_N = (Z(x_1), \dots, Z(x_N))^T$ is a multivariate normal random variable with mean 0 and $N \times N$ covariance matrix K_N , whose entries are $K(x_i, x_j)$. It follows that the simulator output, $Y_N = (y(x_1), \dots, y(x_N))^T$, from inputs X_N is also multivariate normal but with mean $\mu \mathbf{1}$ and covariance matrix $K_N + \sigma_v^2 I_N$, where I_N is the identity $N \times N$ matrix and $\mathbf{1}$ is the N -vector of 1s.

One interpretation is that these assumptions describe a *prior* distribution on all possible functions for the mean M . Different choices for the GP allow for different classes of possible M ; the power of a GP is that these classes can be big enough to allow for all reasonable possibilities. After specifying μ , K , and σ_v^2 , a Bayesian analysis can then be carried out, resulting in a *posterior* distribution for all the functions that can still represent M after accounting for the observed simulator runs.

Another, non-Bayesian, way to think about M and Assumptions A2 and A4 is to think of M as a random function, with μ being a regression function (for example, as in linear regression), and the GP for Z adding errors that are correlated between points. Both formulations have the same mathematical structure but with differing interpretations: the former interprets the GP as a way of modeling M , the latter treats the GP as structured residual error left over from modeling M with a regression function.

Because everything is normally distributed, the predictive distribution for any new run, $y(x_{\text{new}})$, given the observed simulator data $\{X_N, Y_N\}$ is also normal. With

$k_N(x_{\text{new}})$ denoting the N -vector $(K(x_{\text{new}}, x_1), \dots, K(x_{\text{new}}, x_N))^T$ of covariances between the desired prediction and observed data, the mean $\mu_N(x_{\text{new}})$ and variance $\sigma_N^2(x_{\text{new}})$ of the predictive distribution are:

$$\mu_N(x_{\text{new}}) = \mu + k_N(x_{\text{new}})^T (K_N + \sigma_v^2 I_N)^{-1} (Y_N - \mu \mathbf{1}) \quad (3.1)$$

$$\sigma_N^2(x_{\text{new}}) = \sigma_v^2 + \sigma_Z^2 - (k_N(x_{\text{new}})^T (K_N + \sigma_v^2 I_N)^{-1} k_N(x_{\text{new}})) \quad (3.2)$$

Once the correlation function C is specified, parameters $(\mu, \sigma_Z^2, \text{ and } \sigma_v^2)$ can be estimated from the data. For specifying C , the approach taken for deterministic simulators can be adopted here: specify a parameterized family C_θ and use the data to estimate θ , thereby tailoring C to observations. One example for C_θ is the family of squared-exponential correlation functions (also known as the Gaussian kernel):

$$C_\theta(x, w) = \exp \left\{ - \sum_{j=1}^d \theta_j (x_j - w_j)^2 \right\}. \quad (3.3)$$

This correlation function is suited for approximating very smooth, infinitely differentiable, functions over dimension d . Alternative correlation functions exist and are used; one commonly used alternative is the Matérn 5/2 correlation function (Stein, 2012), which is appropriate for approximating less-smooth functions (only 2 derivatives).¹

With a choice of the family C_θ and Assumptions A1-A4, the likelihood of the observed output is available and maximum likelihood estimates (MLEs) $\hat{\mu}$, $\hat{\sigma}_v^2$, $\hat{\sigma}_Z^2$, and $\hat{\theta}$ can be calculated. Henceforth $\mu_N(x_{\text{new}})$ and $\sigma_N^2(x_{\text{new}})$ will be used to denote the mean and variance of the predictive distribution even when the parameters in Equations 3.1 and 3.2 are estimated. The predictive probability distribution for the computer model output $y(x_{\text{new}})$ is then:

$$\hat{y}(x_{\text{new}}) \sim N(\mu_N(x_{\text{new}}), \sigma_N^2(x_{\text{new}})) \quad (3.4)$$

A proper assessment of uncertainty is lost by plugging-in estimated parameters without accounting for their uncertainty. Accordingly, the predictive variance, $\sigma_N^2(x_{\text{new}})$, obtained this way is called the *plugin* (or *nominal*) predictive variance. The alternative of a full Bayesian analysis to estimate the parameters can be computationally impractical in many circumstances, though not impossible; intermediate schemes and approximations have proven to be useful (e.g. Spiller et al., 2014).

For the correlation function in Equation 3.3, and for others such as the Matérn 5/2, the correlation between $Z(x)$ and $Z(w)$ depends only on $x - w$, the difference between the two vectors of inputs. That is, Z is assumed to be a stationary GP (and, consequently, so is y). For functions exhibiting markedly different behavior in one region of input space than in another part, stationarity is problematic. This issue is tackled

¹The Matérn 5/2 correlation function has the form $\left(1 + \frac{\sqrt{5}(x_j - w_j)}{\rho} + \frac{5(x_j - w_j)^2}{3\rho^2}\right) \exp\left(-\frac{\sqrt{5}(x_j - w_j)}{\rho}\right)$. Further discussion of the features of different correlation functions can be found in Chapter 4.2 of Rasmussen and Williams (2006) or Chapter 2.2 of Santner et al. (2018).

and discussed in Gramacy and Lee (2008); Ba et al. (2012); Kersaudy et al. (2015) and Chen et al. (2016), among others.

Despite the fairly complex mathematical expressions above, Gaussian processes are easily accessible thanks to numerous available packages (for example: `DiceKriging` in R (Roustant et al., 2018), the `hetGP` R package (Binois and Gramacy, 2018b) mentioned later, and the `GaussianProcessRegressor` function from `scikit-learn` in Python (Pedregosa et al., 2011)).

In general, a GP is a flexible method for estimating the mean $M(x)$ of the simulator output, despite lack of prior knowledge. This is illustrated in the left-hand panels of Figures 1 and 2, but we first introduce a vital modeling twist to cope with a common feature of stochastic computer simulations.

3.2 Heteroscedastic GP Surrogates

The constant variance of Assumption A1 simplifies the construction of a statistical model because only one intrinsic variance parameter σ_v^2 needs to be estimated. When $\sigma_v^2(x)$ is believed to vary over the input space more must be done. Boukouvalas et al. (2014a) model $\sigma_v^2(x)$ as $\exp(h(x))$ for simple functions h (e.g., polynomials), a simple extension to assuming just one variance parameter σ_v^2 . The exponential transform ensures positivity of the variance. Like analogous approaches to predicting the mean (briefly discussed in Section 3.1), it isn't clear what to use for h , and its simplicity may not meet the complexities found in many applications.

GPs are used for σ_v^2 by several authors (Goldberg et al., 1998; Kersting et al., 2007; Boukouvalas and Cornford, 2009; Ankenman et al., 2010; Binois et al., 2018a). The difficulty is that doing so directly depends on observing $\sigma_v^2(x)$ at the inputs X_n , but these values are not observed. If there are enough replicated simulation runs, r_i , at the inputs x_i , then the sample variances ($s^2(x_i) = \frac{1}{r_i-1} \sum_{j=1}^{r_i} (y(x_{ij}) - \bar{y}_i)^2$, for $i = 1 \dots n$) at the x_i s can be used to estimate the $\sigma_v^2(x)$ at the inputs X_n . Equations 3.1 and 3.2 can then be used to predict $\sigma_v^2(x_{\text{new}})$. (Working with the logarithm of the sample variances and then exponentiating the results avoids negative predictions of the variance.) But this approach, called *stochastic kriging* (SK, Ankenman et al., 2010), is limited by the need for adequate numbers of replicates at each input and the possible inefficiency of treating the variance and mean processes separately.

The limitations can be removed by considering the intrinsic variances at the inputs, $(\sigma_v^2(x_1), \dots, \sigma_v^2(x_n))$, as unknown parameters to be estimated in the same manner as all the other unknown parameters. Goldberg et al. (1998) do so in a fully Bayesian, but computationally taxing, way. Efforts to reduce these costs form the essence of approaches by Kersting et al. (2007) and Boukouvalas and Cornford (2009). A recent variant, proposed in Binois et al. (2018a) along with accessible software `hetGP` (Binois and Gramacy, 2018b), resolves the computational hazards and is the method described and used in this review.

The technical details addressing the computational barriers of a heteroscedastic GP (`hetGP`) have three elements. One, `hetGP` models the log variances as the *mean* out-

put of a GP on latent (hidden) variables. The second uses Woodbury matrix identities (Harville, 1998) to reduce computations from treating all N observations to computations involving only the n unique inputs, a reduction of computational complexity from $O(N^3)$ to $O(n^3)$, especially relevant when there are many replicates. The third element uses MLE to set all parameters.

While full details are provided by Binois and Gramacy (2018a), some specifics of the first element of the description above are worth noting. With $\lambda(x) = \sigma_v^2(x)/\sigma_Z^2$ and $\Lambda_n = (\lambda(x_1), \dots, \lambda(x_n))$ for the n distinct inputs, $\log \Lambda_n$ is taken to be the predictive *mean* of a GP on latent (hidden) variables, $\Delta_n = (\delta_1, \dots, \delta_n)$. For ease of exposition assume the GP has 0-mean (a constant mean is actually the default setting in `hetGP`) and take the covariance function for Δ_n to be $\sigma_g^2(C_g + gR^{-1})$ where $g > 0$, $R = \text{diag}(r_1, \dots, r_n)$, and C_g is a correlation function with parameters θ_g . Then $\log \Lambda_n = C_g(C_g + gR^{-1})^{-1}\Delta_n$. This latent Δ_n approach facilitates smooth estimates of Λ_n and provides a fixed functional form for $\lambda(x)$, but does not incorporate the resulting uncertainty due to the estimates of the intrinsic $\sigma_v^2(x)$ in predictions.

Given Λ_n , the Woodbury identities (Harville, 1998) reduce the likelihood of Y_N , the output at *all* inputs including replicates, to depend on quantities of size n . Maximum likelihood estimates for the unknown parameters can then be computed at a cost of $O(n^3)$. Derivatives are also computable at a cost of $O(n^3)$, further facilitating optimization.

Fish Example. We apply the homoscedastic GP (`homGP`) and `hetGP` surrogates to the fish example from Section 2.2. The simulation budget is constrained to 400 runs and focuses on the relationship between the total number of fish in a population and the number of fish that are recaptured in the second round of capture. The total population is assumed to be any integer between 150 and 4000. The simulator is run 20 times at each of 20 unique x locations, uniformly chosen in that range. Applying a `homGP` surrogate with a Matérn 5/2 correlation function produces the results in the left panel of Figure 1; the right panel shows the results of `hetGP`. The mean number of recaptured fish decreases rapidly between $x = 150$ and $x = 600$, after which the decrease is at a slower rate. This is clearly a non-linear relationship, and the Gaussian process captures the mean trend quite well. However, the predictive variance of the `homGP` in the left panel appears too large for large values of x , and too small for small values of x . This is perhaps a minor issue here, but it suggests that assuming constant intrinsic variance is not reasonable. For `hetGP`, the estimated intrinsic variance, $\sigma_v^2(x)$, becomes smaller as x gets larger; going from 39.1 when $x = 150$ to 5.9 when $x = 4000$. This is reflected in the predictive variance for `hetGP` in the right panel. For this example, the mean predictions are quite similar for both surrogates, but the predictive variances are different.

Ocean Example. For the ocean example (Section 2.3), we take each simulation run to be the mean of 6 simulation runs (the true simulator is known to be non-normal, this

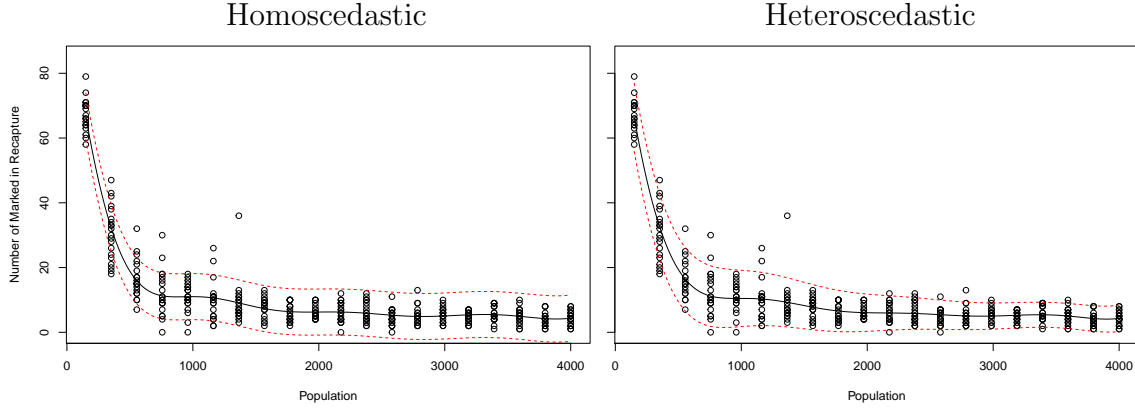


Figure 1: Summary fits to 400 simulations of the fish model, 20 replicates at each of 20 population sizes (uniformly spaced in $[150, 4000]$ then rounded down to nearest integers). The left panel shows the use of homGP via the mean of its predictive distribution, μ_N , the black line; the red dashed lines form the 95% (plugin) uncertainty intervals based on σ_N^2 . The right panel exhibits the same for hetGP.

fix makes the example more straightforward). We also fix the two diffusion coefficients, K_x and K_y , at the values 700 and 200, leaving the two spatial coordinates as the only varying inputs. Using 1000 simulations (50 unique locations each replicated 20 times), we obtain the predictive mean surface and the predictive standard deviation surface (that is, the surface of standard deviations of simulator output, which includes both the uncertainty around the predictive mean and the estimate of σ_v^2 , the intrinsic variance). The surfaces are plotted in Figure 2, with the left column for homGP and the right column for hetGP. The mean surfaces for both estimators (top row) show high oxygen concentration in horizontal bands coming from the West, and low oxygen concentration in the South East. The predictive standard deviation for homGP (bottom-left) is relatively constant across the input area (clearly affected by the constraint that σ_v^2 is constant). The minor increases on the boundary results from increases in the uncertainty of the mean. The standard deviation surface for hetGP is markedly different, and so the intrinsic variance is most likely non-constant. The numerical results in Section 4.3 provide further evidence that the intrinsic variance is non-constant; but they also imply that the hetGP intrinsic variance estimates here may be inaccurate.

3.3 Non-Normal Variability

In many applications assuming normally distributed variability v is inappropriate. For example, count data, as in Sections 2.1 and 2.2, are non-normal. Transformation of the data is a time-honored device that sometimes induces “enough” normality to allow its use. For example, Henderson et al. (2009) uses the logit transformation ($\log p/(1-p)$) in analyzing the proportion of deletions in mitochondrial DNA. In Plumlee and Tuo (2014) a different route is taken by focusing on the quantiles of the output distribution

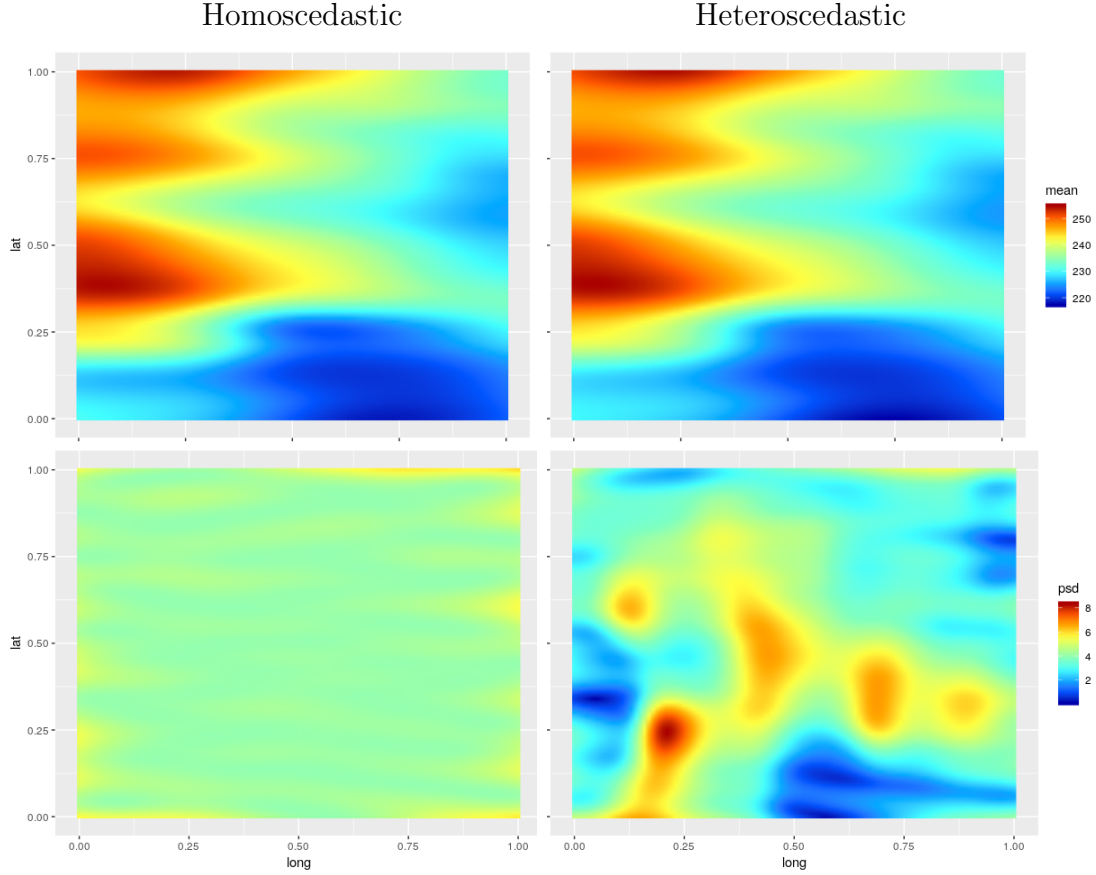


Figure 2: Summary fits to 1000 simulator runs consisting of 20 replicates at each of 50 input locations from a maximin Latin Hypercube Design (defined in Section 4) of size 50 in 2 dimensions. The top row provides predictive means, μ_N , and the bottom gives standard deviations, σ_N , of the predictive distribution of oxygen concentration. The left column uses homGP, the right uses hetGP.

— normality is not needed. Both of these approaches have the appeal of leading to relatively simple modifications of the methods in Sections 3.1 and 3.2. There are also more complex methods that generally lack the same ease of implementation. For example, Moutoussamy et al. (2015) attempt to model the underlying probability density function itself, rather than the output y . Xie and Chen (2017) devise a Student t -process that is not much different than the GP process while at the same time allowing heavier tails in the distribution of the data.²

²hetGP also implements a Student- t variant (Wang et al., 2017; Shah et al., 2014; Chung et al., 2019).

3.3.1 Quantile Kriging

The Quantile Kriging (QK) method introduced by Plumlee and Tuo (2014) directly models specific quantiles of interest, such as the median and the lower/upper 95% quantiles at each input. Minimal assumptions about the distribution of the simulator output are required, instead, $Q_q(x)$, the q^{th} quantile of the simulator output at input x , is modeled with a GP. Given values $Q_q(x_i)$ at inputs x_1, \dots, x_n , the quantile, $Q_q(x_{new})$ for x_{new} , can be predicted using Equations 3.1 and 3.2.

To implement QK, values of the targeted quantiles at the inputs are needed. Just as in Section 3.2, where sample variance estimates at the inputs can be used, sample quantiles can be used here. Said sample quantiles are calculable given enough replicates r_i at each x_i . The GPs used to predict new quantile values, $Q_q(x_{new})$, should also include a noise term σ_q^2 to acknowledge that the sample quantiles are estimates.

A useful modification incorporates the quantile q as an additional input to the GP model. The quantile $Q_q(x)$ is reformulated as $Q(x, q)$ and the dimension of the problem increases from d to $d + 1$. This strategy, allowing for the prediction of $Q(x, q)$ for any desired quantile q , not just those that were empirically estimated, is used by Fadikar et al. (2018) for the Ebola model. A variant of QK called Asymmetric Kriging (AK, Zhang and Xie, 2017) leverages quantile regression methods (Koenker and Bassett Jr, 1978) and does not require sample quantiles, but is not as effortlessly implemented as QK.

Fish Example. For the fish simulator, QK is easily implemented with the same simulated dataset as before since many replicates are available. The modification using quantile q as an added input dimension is adopted here. The sample 2.5%, 27.5%, 50%, 72.5% and 97.5% quantiles at each of the 20 population sizes form the observed data. The plot in Figure 3 exhibits 5 projections (one for each of the listed quantiles) of the predicted mean surface of $Q(x, q)$. The center black dashed curve in Figure 3 is

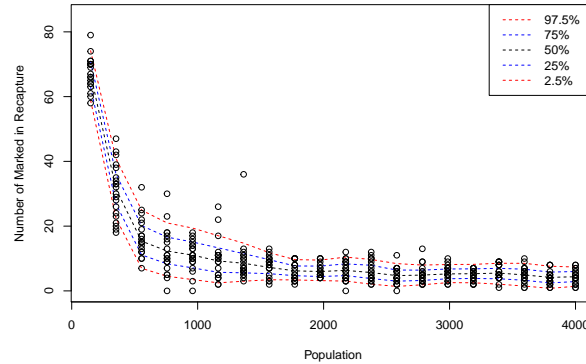


Figure 3: Same setup as Figure 1 but with a QK surrogate. Mean predictions of 5 quantiles (2.5%, 25%, 50%, 75% and 97.5%) are provided.

the predicted median. The 95% intervals are in red, and the 50% intervals are in

blue. The non-monotone “wavy” lines for the 2.5% and 97.5% quantiles reflect the natural variability of sample quantiles based on only 20 observations for those extreme quantiles; the other quantiles exhibited display the expected regularity.

3.4 Multiple Outputs

The discussion thus far has assumed that the simulator outputs a single scalar quantity of interest. If there are multiple outputs, each can be treated independently with its own surrogate model. Doing so ignores any correlation between different outputs, which is a waste of available information; this is particularly a problem if the output is a time-series. One alternative is to treat the index, t of the T outputs, as an additional dimension to existing inputs, changing the dimension of input space from d to $d + 1$. If there are N simulator runs then the number of data points becomes NT . GP surrogates then require the inversion of $NT \times NT$ correlation matrices, and when NT is large, this can pose a high computational barrier. More sophisticated approaches, building multivariate GPs, have been employed (Conti and O’Hagan, 2010; Fricker et al., 2013; Paulo et al., 2012).

A different, widely used approach, is to reduce the effect of the size of T to a smaller K_0 by representing the output through the use of basis functions, $\psi(t)$:

$$y(x, t) = \sum_{k=1}^{K_0} w_k(x) \psi_k(t) + \delta(x, t). \quad (3.5)$$

Coefficients $w_k(x_i)$ $k = 1, \dots, K_0$ are determined by the data; and $\delta(x, t)$ is the residual error between the basis function representation and the data y . If $K_0 = T$ then $\delta = 0$. Typically, K_0 is taken to be much less than T but large enough so that the error, δ , is sufficiently small.

A common choice of basis functions are principal components: the ψ s are the eigenvectors of the matrix $Y^\top Y$, the first K_0 of which are in correspondence with the first K_0 eigenvalues in decreasing order. It is often the case that the first few (five or less) principal components are enough to capture sufficient information about the full (T) data set. Coefficients $w_k(x_i)$ are then equal to $\sum_{t=1}^T y(x_i, t) \psi_k(t)$. More information about principal components can be found in Jolliffe (2011) and software for obtaining ψ and w_k is prevalent.

Each $w_k(x)$ can be independently modeled with a surrogate and predictions for $y(x, t)$ can then be obtained from Equation 3.5, ignoring δ . Further discussion about using principal components to model high-dimensional simulator output can be found in Higdon et al. (2008). Principal components are utilized in Fadikar et al. (2018) to model the time-series output of the stochastic Ebola simulator (Section 2.1).

The choice of basis function can be important: it is essential that key features of the data set are captured by the basis representation, and not left within the discarded $\delta(x, t)$. For example, if the goal is to calibrate input parameters (see Section 5), Salter

et al. (2019) advise against principal components and suggest an alternative. Specialized bases may be appropriate when t is time. For example, Bayarri et al. (2007a) use wavelets for the ψ_k s albeit in a deterministic setting. A more tailor-made, complex solution regarding time-series might be desirable, and efforts at this have been made (Farah et al., 2014; Sun et al., 2019). These depend on formulations and assumptions about the time dependencies in $y(x, t)$ and are strongly reliant on specifics of the problem as distinct from the generality of the techniques described above.

4 Experimental Design

For an experiment, the design (the choice of x values) and analysis (the assessment of the output $y(x)$) are, in principle, closely connected. With a goal say, of predicting the simulator’s output and a criterion to assess how well the goal is met, such as the average prediction uncertainty (the integrated mean-squared prediction error, IMSPE³), one can seek designs to optimize the criterion. Since the criterion (and the design) will usually depend on a surrogate, which in turn depends on unknown parameters, what to use as a stand-in for the parameters before any data are collected is an issue. Extensive study of single-stage deterministic computer experiments, DCE, resolved this dilemma by downplaying optimality and recommending readily computed “space-filling” designs, designs where no large region of input space is missed. Space-filling designs are readily computed, whereas optimizing IMSPE is complicated and without substantial advantage. For practical adoption designs need to be easy to produce as well as effective.

Multiple methods exist for obtaining space-filling designs, the most popular being Latin hypercube designs (LHDs) (McKay et al., 1979).⁴ LHDs have proved adequate, especially when enhanced with an additional criteria, such as the maximin criteria, where one also maximizes the minimum distance between points in the design.⁵ Even a random LHD will often suffice. Sobol sequence designs (Sobol, 1967) are equally effective for predicting the output of a deterministic simulator. The x s for Sobol designs are generated sequentially making it easy to retain the space-filling character when a multi-stage or sequential design strategy is used.⁶ Pronzato and Müller (2011) have a lengthy discussion of these and other space-filling methods, some pertinent to non-rectangular geometries.

For stochastic simulators the picture is less clear. The presence of intrinsic variability raises the complication of replication, not present in DCEs. Replicates obviously

³With $\sigma_N^2(x)$, the predictive variance, the IMSPE, of a design D is equal to $\int_{x \in X} \sigma_N^2(x) dx$

⁴A Latin hypercube design is one where: on each dimension, the input space is divided into, usually, equal intervals and each interval is constrained to contain exactly one data point.

⁵Such maximin LHDs are produced for example, by the maximinSLHD function of the *R* package SLHD (Ba, 2019), or the lhs function from the Python package pyDOE (Lee, 2015)

⁶In *R*, the sobol function in the *R* package randtoolbox (Yohan Chalabi and Wuertz, 2019) can be used to generate Sobol sequences.

have an effect on the estimation of the intrinsic variance, σ_v^2 , and therefore on prediction (see Section 3.2), and so the number and location of replicates are important. A simple approach for a single-stage experiment is to use a space-filling design to establish the sites $X_n = (x_1, \dots, x_n)$ of the experiment and then add replicates at each site. Determining the number, r_i , of replicates at each site x_i and how to apportion between replicates and sites, that is, how to choose the number of unique sites, n , given a total simulation budget N , is not well understood. In fact, there is limited theoretical evidence of the need for replicates altogether, although there is numerical evidence and wide belief that replicates can be advantageous. For example, Wang and Haaland (2018) produce designs by minimizing bounds on IMSPE. Their numerical results show no need for replicates unless $\sigma_v^2(x)$ is large compared to σ_Z^2 (a factor in measuring uncertainty in estimating the mean M).

The presence of intrinsic variability suggests there is value in multi-stage designs where stage 1 is used to get information about $\sigma_v^2(x)$ and later stages exploit this information to allocate replicates and select new inputs. Questions arise as to how inputs should be selected for stage 1, and also how to leverage the results from stage 1 to select new inputs and replicates in later stages. The two factors, replication and multiple stages (including fully sequential), are central to developing adequate design strategies. Attention is paid to both factors in the discussion below.

4.1 Single-Stage Design

A common approach in single-stage studies is to use space-filling designs for inputs, say n in number, and r replicates at each input, sometimes with no repeats i.e., $r = 1$. Predictions follow as described in Section 3 depending on the particular prediction model selected. Choices have to be made about the total number of runs and the number of replicates at each input site ($N = nr$). Often, N is a question of budget, but there is little insight into how r should be chosen except when meeting a specific surrogate model requirement, as in SK (Section 3.2).

For their single-stage study, Marrel et al. (2012) use a standard LHD with no repeats to compare the performance of different statistical models. On the other hand, Plumlee and Tuo (2014) use a LHD design with varying numbers of replicates r_i at each x_i . In their case, the number of replicates *must* be large, because the QK method (Section 3.3.1) depends on computing quantiles of the output $y(x_i)$ at each input in the design.

4.2 Two-Stage Design

As noted above, the case for a two-stage design is largely to enable estimation of σ_v^2 at stage 1 and use it to make sound choices for the second stage. Ankenman et al. (2010) provide one solution in the context of SK. A first-stage design chooses the x_i s via an LHD of size n_1 with a common number, r , of replicates at each of the inputs, resulting in a total number of $N_1 = n_1 r$ runs at stage 1. The first-stage analysis uses the r replicates at each input to estimate $\sigma_v^2(x_i)$ using the sample variances. As outlined in

Section 3.2, a GP (working with $\log s^2(x_i)$) is then used to produce a moment-based “plug-in” estimate of $\sigma_v^2(x)$ for all x . A different GP uses that variance estimate and builds a predictor for the mean output M .

For stage 2, n_2 additional unique input locations are chosen so that the combined set of design locations, $X_n = (x_1, \dots, x_n)$, remains space-filling. The IMSPE is then calculated by integrating the MSPE over all possible inputs X using the GP model constructed in stage 1. Minimizing the IMSPE with respect to the number of replicates $R_n = (r_1, \dots, r_n)$ provides the optimal number of replicates for the chosen X_n . Details are in Ankenman et al. (2010).

In this setting, a Sobol sequence could be used to obtain a design that is space filling at both stage 1 and stage 2. This is not what is done in Ankenman et al. (2010), but a Sobol sequence is easier to implement and likely to yield similar results. Choosing the unique inputs X_n for stage 2 by optimizing the IMSPE could also be done, but adds to the computational burden. Suitable recommendations for the values of n_1, n_2, N and the replicates at each distinct input are lacking (in Ankenman et al. (2010) the recommendations are ad hoc) and, as for one-stage experiments, open for study. A third-stage design (or indeed, any multi-stage design) can be constructed by repeating stage 2 in the above process.

4.3 Sequential Design

When the statistical design and resulting analysis are closely coordinated, it may be feasible to carry out a sequential process whereby, after the first stage, a run is chosen one-at-a-time. After each run all quantities of relevance can be updated in order to determine the next run. This addresses the issue of learning about σ_v^2 and obtaining new runs without pre-specifying their allocations. An advantage of a sequential design is the possibility of stopping when a criterion is met before a budget constraint is reached. Another advantage is the increased likelihood of making useful runs of the simulator, replicates or otherwise. For some objectives, such as optimization (Section 6.3), a sequential design is usually essential. For global prediction, Binois et al. (2018b) present an implementable approach to sequential design — the previously mentioned `hetGP` package has an implementation.

The strategy in Binois et al. (2018b) begins at stage 1 with a space-filling design D_1 of n_1 inputs and an allocation of runs $(r(x_1), \dots, r(x_{n_1}))$. Using a GP for M and a latent GP prior on σ_v^2 , as in Section 3.2, a MLE computation deals with all parameters, leads to predictors, and a calculable estimate of $\text{IMSPE}(D_1)$. A new point z is considered, either as a new unique input x_{n_1+1} or as a replicate of an existing input in D_1 . Selection z is added to the design D_1 if z minimises $\text{IMSPE}(D_1 + z)$, yielding a new design D_2 . This myopic rule can be iterated and each time a new point is added the surrogate, including MLEs of its parameters is updated. The process stops when a criterion is met or the computational budget exhausted.

Computational viability is strained by the updating required after each run. On the other hand, the computational burden is eased by nature of it being “greedy”: it

only seeks the optimal data point for the very next simulator run, ignoring runs that may be better in the long run.

This is not the only sequential design scheme available for global prediction problems. For example, the tree-generating processes used in TGP and BART (see Section 6.1) deliver specialized sequential design strategies. Details are available in Gramacy and Lee (2009) and Chipman et al. (2010).

When fully sequential methods are feasible the seqhetGP strategy sketched above is valuable. There are several aspects worth examining:

- The extensive use of a statistical model in the construction of the design requires additional scrutiny of the chosen model; for example, by diagnostics that assess the quality of the surrogate.
- The first stage of a fully sequential strategy needs study lest a poor (e.g., too small) initial design lead to a poor starting surrogate model, leading to a sequence of poor choices thereafter.
- The utility of a sequential design depends on the cost of implementation compared to the cost of simulator runs. For challenging problems simulator runs are likely to be costly enough to make sequential design attractive.
- There may be modifications to a sequential design that reduce computational load without paying a significant cost in accuracy. For example, periodic re-estimation of parameters may be adequate rather than re-estimating all parameters after each step.

Fish Example. We apply the seqhetGP scheme to the Fish simulator with the first-stage design a maximin LHD of 10 locations in $[150, 4000]$, each with 5 replicates. As before the total budget is 400 runs. The resulting data set and hetGP predictions are in Figure 4. Some new sites are chosen and replicated heavily, others less so. One input, $x = 1283$, was run 33 times. The predicted mean looks the same as before (Figure 1) but the intrinsic variance is more nuanced: it no longer simply decreases as x increases. Now it is estimated largest when $x = 609$, where the intrinsic variance is 41.0, and declines to $\sigma_v^2(150) = 28.5$, and $\sigma_v^2(4000) = 5.1$. Smaller intrinsic variance for low x makes sense, since a large percentage of the fish will be recaptured. When x is large the number of recaptured fish will almost certainly be small, again leading to smaller intrinsic variance.

Ocean Example. The sequential design for the Ocean simulator has an initial design of 50 sites, chosen by a maximin LHD in $2-d$, each site with 5 replicates. The remaining 750 data points are assigned via the sequential scheme. Mean and standard deviation surfaces are in Figure 5. For the standard deviation surface, the design sites are superimposed along with the number of replicates taken at the sites. The mean surface in the left panel is somewhat different than for the non-sequential analyses (Figure 2,

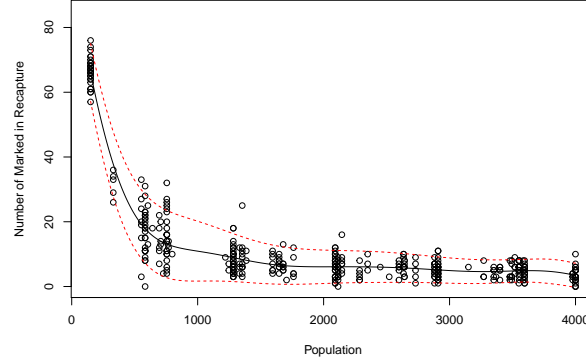


Figure 4: Using the hetGP surrogate under a seqhetGP design for the fish experiment: the black line is μ_N , the mean of the predictive distribution; the red dashed lines form the 95% (plugin) uncertainty intervals based on σ_N^2 .

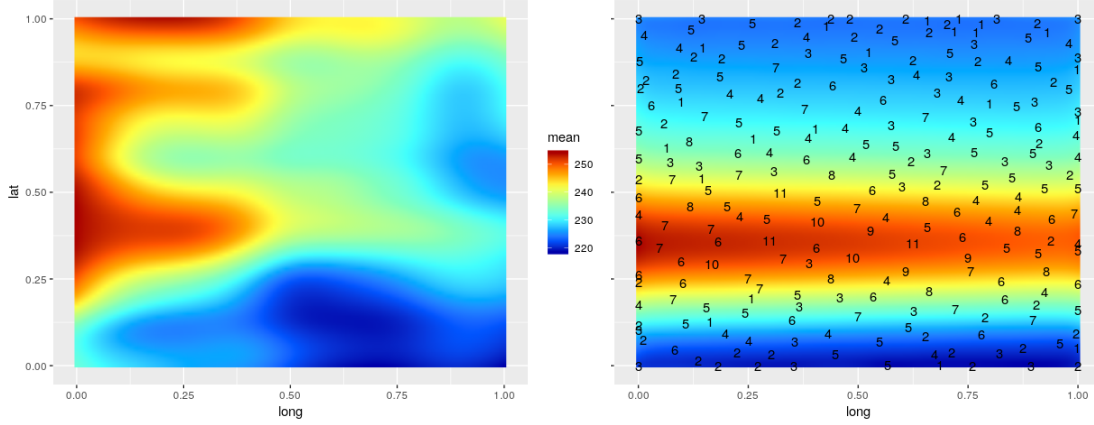


Figure 5: Using the hetGP surrogate under a seqhetGP design for the fish experiment: the left plot is the mean, μ_N , of the predictive distribution; the right plot is its standard deviation, σ_N . Design sites with their replicates are superimposed on the right-hand plot.

top row) but not dramatically so. But, as evident in the figures, the standard deviation surfaces are substantially different. For the sequential design, the added inputs (to the initial design) have been heavily replicated in regions where the standard deviation is large, and not so in regions where the standard deviation is small. In comparison, the non-sequential design wasted many replicates in regions where the standard deviation is small.

A telling comparison of the three different Ocean model surrogates is their out-of-sample predictive performance. By choosing, via a LHD, 500 new sites, surrogate predictions at these 500 test sites can be made. Then, performing many replicate runs (up to 100,000) at each site, the “true” mean can be taken as the sample mean from the highly replicated test site data. The mean squared error, MSE, (the average squared

difference between the surrogate’s prediction of the mean and the “true” mean) can be calculated as a measure of the surrogate’s predictive capability. The smaller the MSE, the better the surrogate.

Another measure is the proper scoring rule from Equation 27 in Gneiting and Raftery (2007) which provides an overall measure of accuracy for the surrogate, testing the accuracy of both the mean and variance predictions, with higher values being better. For a set of out-of-sample input points x_1, \dots, x_p and simulator output values y_1, \dots, y_p , with respective surrogate predictive mean values $\mu_N(x_1), \dots, \mu_N(x_p)$ and predictive variances $\sigma_N^2(x_1), \dots, \sigma_N^2(x_p)$; the score is:

$$\sum_{i=1}^p \left(- \left(\frac{y_i - \mu_N(x_i)}{\sqrt{(\sigma_N^2(x_i))}} \right)^2 - \log(\sigma_N^2(x_i)) \right). \quad (4.1)$$

In the case of Gaussian predictors, the score is equivalent to the predictive log likelihood. Table 1 shows the results of this comparison. The numerical results in Table

	homGP	hetGP	Seq hetGP
MSE	0.0397	0.0370	0.0257
Score	0.543	0.702	0.720

Table 1: Performance results of the three ocean model surrogate model fits: mean squared error of prediction (MSE) at 500 test locations (lower numbers are better); proper score at the same test locations (higher numbers are better).

1 and the plots in Figures 2 and 5 suggest that mean predictions are similar whether using homGP or hetGP with a fixed design, but are inferior to those from hetGP with a sequential design. Moreover, the score numbers and the standard deviation surfaces in those figures indicate that heteroscedasticity is indeed present and the prediction problem is best handled using the sequential design.

4.4 Designing for Statistical Model Parameter Estimation

The discussions in Sections 4.2 and 4.3 construct designs that rely on a statistical surrogate model based on stage 1 data in order to choose subsequent data points. The quality of the designs depends on the accuracy of the statistical model which, in turn, depends on the accuracy of its parameters. An alternate approach to those used in Sections 4.2 and 4.3, is to construct an initial design with the express purpose of better estimating these parameters.

Boukouvalas et al. (2014a) address this problem. They focus on hetGP models, using a simple parametric function for the variance ($\sigma_v^2(x) = \exp(h(x))$, where h is a simple function (e.g., a polynomial with coefficients β)). They propose choosing designs that maximize a criterion previously used for deterministic simulators by Abt and Welch (1998): the logarithm of the determinant of the Fisher information matrix,

$\log |I|$. Numerical results suggest this method gives improvements in estimating the parameters, but overall global prediction is no better, and sometimes worse, than using a space-filling design. With prediction the final goal, the question arises about how to make use of such designs for stage 1 in a multi-stage or sequential setting, where its impact on obtaining better initial surrogate models can be felt. For example, see Zhang et al. (2020).

5 Calibration

Calibration is needed when there are inputs to the simulator that are neither known nor measurable, a common condition in practice. Transmissibility in the Ebola simulator or the diffusion coefficients in the ocean model are examples of such inputs. In order to infer (indirectly) values for these inputs and produce predictions, added information in the form of field data (experimental or otherwise) are necessary. Inclusion of field data and calibration parameters, labelled u_C , leads to an expanded version of the basic model from Equation 1.1:

$$y_F(x) = y_S(x, u_C) + \epsilon, \quad (5.1)$$

where y_S is a simulator with x the controllable (or directly measurable) inputs and u_C the unknown non-measurable inputs, $y_F(x)$ are real-world field observations at x , and ϵ is measurement error associated with $y_F(x)$ with variance σ_ϵ^2 .

The formulation in Equation 5.1 implies that the simulator y_S is a true representation of the reality observed by y_F , but with observation error. In actuality, the simulator is only an approximation and the discrepancy (bias) between y_S and reality must also be accounted for, leading to the representation

$$y_F(x) = y_S(x, u_C) + \delta_{MD}(x) + \epsilon \quad (5.2)$$

where $\delta_{MD}(x)$ is the model discrepancy between simulated and “true” output at x .

Multiple competing methodologies and philosophies exist for calibration. Despite its significance and prevalence, no satisfactorily comprehensive comparison between different methods has been conducted, for either deterministic or stochastic simulators. This section outlines several refined solutions to the calibration problem; a comprehensive comparison awaits study.

5.1 Kennedy-O’Hagan Calibration (KOH)

The formulation in Equation 5.2 was made by Kennedy and O’Hagan (2001) for deterministic simulators and is the basis for much of the calibration and related prediction work since. The formulation is also appropriate for stochastic simulators, the only difference being the type of surrogate used. The strategy pursued by Kennedy and O’Hagan (2001) as implemented in Bayarri et al. (2007b) obtains a surrogate for y_S and models $\delta_{MD}(x)$ with a GP (a GP allows for flexible modeling of the discrepancy).

After replacing y_S by a surrogate, posterior distributions for all unknowns can be obtained via a Bayesian analysis. In practice, the surrogate model is typically fit separately using only the simulator data, ignoring possible influences from the field data. Details and discussion of this modular approach can be found in Bayarri et al. (2007b) and Liu et al. (2009).

The KOH approach emphasizes the necessity to address calibration and model discrepancy together. Confounding between u_C and $\delta_{MD}(x)$ inevitably occurs because there are multiple combinations of u_C and $\delta_{MD}(x)$ that result in the same observed field data. u_C is thus non-identifiable and its estimation is compromised. However, by taking into account the bias, $\delta_{MD}(x)$, the resulting *predictions* for y and $E(y)$ are sound even if the individual estimates for u_C and $\delta_{MD}(x)$ aren't. For details and further discussion see, for example, Brynjarsdóttir and O'Hagan (2014) and Tuo and Wu (2016).

Multiple attempts to circumvent the confounding have surfaced. Tuo et al. (2015) alleviates the ambiguity in u_C by formally defining it as a least-squares quantity; Gu and Wang (2018) propose novel priors for the discrepancy that compromise between the Tuo et al. (2015) strategy and KOH; and Plumlee (2017) introduces priors on the discrepancy that are orthogonal to the prior mean. In the stochastic simulator literature, Oakley and Youngman (2017) removes $\delta_{MD}(x)$ but compensates by inflating the variability in the prior distribution for u_C . Ignoring $\delta_{MD}(x)$ altogether, and working solely with Equation 5.1, can be justified by strong evidence of the simulator being accurate, but such evidence is rare.

Revisiting Ebola. The Ebola ABM study (Fadikar et al., 2018) is an example of a stochastic simulator being calibrated using the KOH framework. The simulator has 5 unknown, unmeasured inputs u_C and the output is the log of the cumulative number of infected individuals up to week 1 and every week thereafter up to 57 weeks. Field data, a set of actual reported cumulative counts, is also available. For the statistical model, the QK strategy in Section 3.3.1 is followed. Time-series output trajectories are reduced to a more manageable 5 dimensions using the principal component decomposition outlined in Section 3.4. The KOH formulation is followed to provide posterior distributions for the unknowns u_C and $\delta_{MD}(x)$, which are then used to make predictions of the cumulative counts (and other quantities). For the model discrepancy, a highly specified Gaussian spline is used rather than a GP. In the main analysis, which restricts the field data to only the first 20 weeks, the estimate of model discrepancy is almost zero. A subsequent analysis done using field data up to week 42 exposes some inaccuracy of the simulator (non-zero $\delta_{MD}(x)$) — the simulator continues to predict infections, even after the epidemic has died in reality.

Ocean Example. The previous Ocean analyses fixed the 2 diffusion coefficients. Realistically, they are unknown and thus calibration is necessary. We create fake “field” data by running the simulator at 150 different longitude-latitude coordinates using the previously fixed values of the diffusion coefficients ($K_x=700$, $K_y=200$) as the

true values. To these, we add normally distributed pretend “observation error” with a standard deviation of 2. In real problems, the field data would be observed and not generated like this. Note also that there is *no* model discrepancy in this constructed problem.

With the diffusion coefficients now uncertain, the simulator has 4 inputs. A computer experiment is designed with runs at the 150 sites used for the field data and 500 unique selections of the calibration parameters K_x and K_y . This is done by combining copies of the 150 longitude and latitude sites with a 500 maximin LHD for (K_x, K_y) , and then improving the combined design by maximizing the minimum distance between design points in the 4-dimensional space. Call this set of points D_{oc} . The simulator experiment is carried out by taking 10 replicates at each point in D_{oc} . Surrogates, homGP and hetGP, are fit with this fixed design. In addition, a hetGP surrogate is constructed using a sequential design, where the initial design consists of only 4 replicates of D_{oc} and the remainder of the budget is then assigned following the strategy of Binois et al. (2018b) described in Section 4.3.

For a KOH analysis done in modular fashion, the surrogates are fit only using the simulated data. MCMC is then used to obtain posterior distributions for the remaining unknowns (the diffusion coefficients, K_x and K_y ; the variance and correlation parameters of the model discrepancy GP, σ_{MD}^2 and θ_{MD} ; and the observational error, σ_ϵ^2). The posterior distributions for the key parameters are in Figure 6. The true values for the unknowns are $K_x = 700$, $K_y = 200$, $\sigma_{MD}^2 = 0$ and $\sigma_\epsilon^2 = 4$.

For all three surrogate models, the posterior distributions for K_x are fairly diffuse, and the K_y posteriors are more concentrated. None are particularly accurate. All surrogates incorrectly place weight for the discrepancy on values away from 0. None of the estimates of observational error are accurate either, possibly a reflection of the non-zero estimate of discrepancy. These plots may be an example of confounding between the parameters and underline the dilemma of calibration: obtaining accurate values of calibration (and other) parameters in the possible, let alone actual, presence of model discrepancy is problematic. However, KOH can produce effective posterior predictive distributions. Table 2 compares predictions by KOH calibration with 3 other calibration approaches, all of which specify 0-discrepancy. The first one estimates K_x and K_y by least squares (LSE): (K_x, K_y) is chosen such that the sum of the squared residual difference between the mean surrogate prediction and the observed data is minimized. New observations are then predicted by running the surrogate with the parameters (K_x, K_y) replaced by the least squares estimates (\hat{K}_x, \hat{K}_y) . The second approach follows a frequently adopted practice by guessing, or “judiciously selecting”, specific values for K_x and K_y . Here, the choices $K_x = 400$ and $K_y = 500$ are made. We call this method SINGLE. The third method, NOCAL, generates predictions as if there was no field data, and the distribution for (K_x, K_y) is taken as their prior distribution, independent uniform priors on $[100, 1000]$. For both NOCAL and KOH a distribution for the oxygen concentration is obtained by sampling values of K_x and K_y (for NOCAL from their prior distribution, for KOH from their posterior distribution) and plugging them into the surrogate.

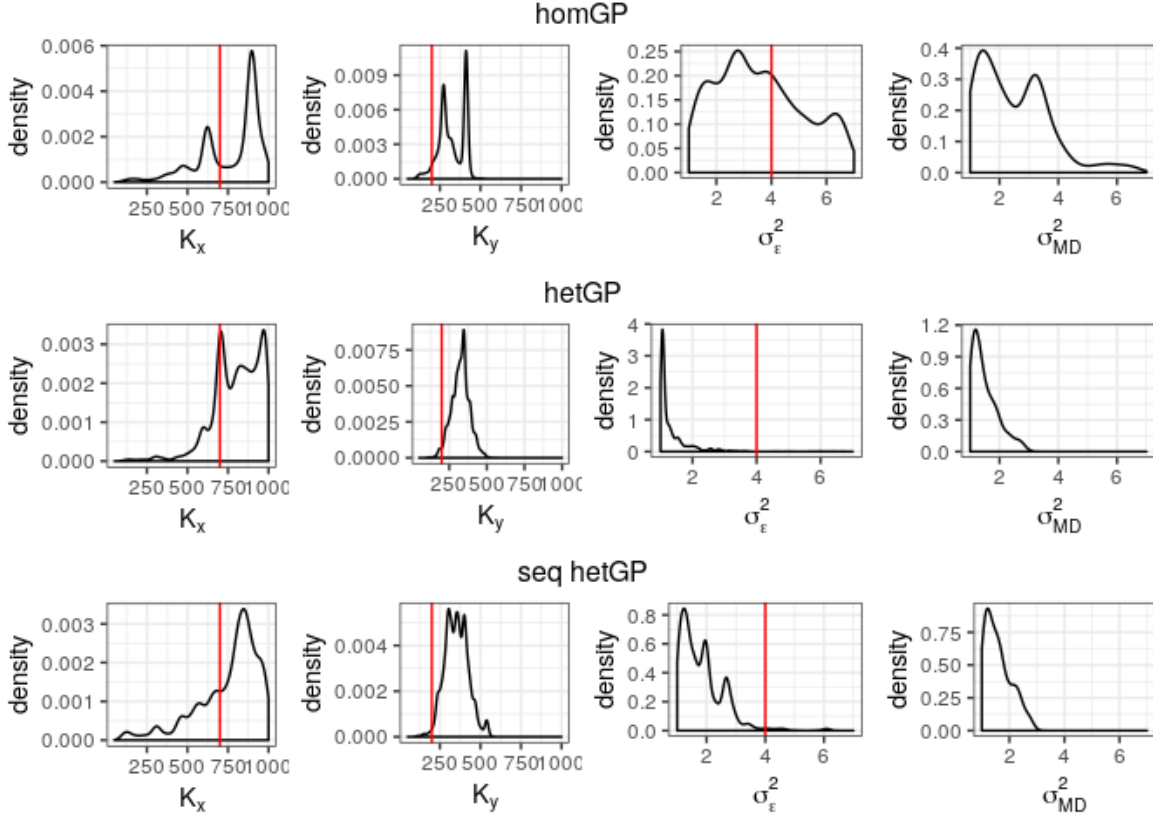


Figure 6: Calibration results for the Ocean model. The top row shows the posterior densities for the four parameters using the homGP surrogate with the fixed design, the middle row uses the hetGP surrogate with the fixed design, and the bottom row uses the hetGP surrogate with the sequential design. The budget for both the fixed and sequential design is 5000 runs. The true values are superimposed as red vertical lines.

The main conclusion is that LSE and KOH are equally effective and both better than SINGLE and NOCAL. The mean predictions (MSE) from LSE are marginally better than KOH, but overall (score) KOH typically performs better than LSE. By both metrics, SINGLE and NOCAL produce worse predictions. Additionally, it is possible that the variability in LSE, SINGLE, and NOCAL is understated, not only because discrepancy is ignored, but because the observational error variance is taken as known while in KOH it is estimated (and thus the score values for LSE, SINGLE and NOCAL are perhaps overly flattering). For the three surrogates, few differences appear, although the homGP surrogate does seem the worst. An interesting observation here is that the least squares estimates (\hat{K}_x, \hat{K}_y) are not always close to the true values, perhaps due to imperfections and high variability in the surrogate, or effects from the specific designs. The differences in the posterior distributions for (K_x, K_y) in the left panels of Figure 6 might also reflect the same uncertainties. What does emerge is that even when model discrepancy is absent, KOH produces predictions as good as

		(\hat{K}_x, \hat{K}_y)	LSE	SINGLE	NOCAL	KOH
MSE	homGP	(1000, 298.4)	83.9	85.4	85.6	84.1
	hetGP	(1000, 309.5)	83.9	85.5	85.5	84.0
	Seq hetGP	(992.0, 316.8)	83.9	85.6	85.5	84.2
Score	homGP		-2.53	-2.62	-2.63	-2.55
	hetGP		-2.48	-2.53	-2.56	-2.39
	Seq hetGP		-2.46	-2.50	-2.52	-2.38

Table 2: Performance results of the three ocean model surrogates under KOH calibration. MSE at the 500 test locations and “true” values used for Table 1; similarly for proper score. (\hat{K}_x, \hat{K}_y) are the least squares estimates for (K_x, K_y) , LSE presents the predictive results from least squares calibration, SINGLE the results from arbitrarily choosing (750, 185) for the diffusion coefficients, NOCAL the results from sampling from the prior for (K_x, K_y) , and KOH the results from performing KOH calibration.

LSE, which is reassuring. The danger in arbitrarily specifying a single value for the calibration parameters (SINGLE) seems clear, although this too may be affected by the several uncertainties. An important note to mention here, is that the presence of intrinsic noise lowers the value of field data, reducing the information contained within any one field observation about the calibration parameters. This can make it difficult to effectively calibrate noisy stochastic simulators without an abundance of field data.

The focus here, consistent with Section 4, has been on improving global prediction. If the problem is instead to provide good estimates for calibration parameters when model bias is absent, then different designs may be better suited. Damblin et al. (2018) address this in the context of deterministic simulators, but it is unclear how such methods extend to stochastic simulators.

5.2 History Matching (HM)

History Matching is an alternative calibration method that has been used on complex deterministic simulators (Craig et al., 1997; Vernon et al., 2010) to seek simulator inputs with outputs that closely match observed data, while recognizing the presence of the various uncertainties (including model discrepancy). The HM philosophy is to rule-out “implausible” inputs, rather than find probable inputs, and to do so in a comparatively simple way. The process can be repeated in so-called “waves”, using non-implausible inputs found at one wave to generate simulation runs for the next wave. HM aims to not waste effort exploring regions of inputs where u_C is unlikely to lie. Andrianakis et al. (2017) applies HM to a stochastic simulator in a context where there are 96 inputs and 50 outputs. Multiple outputs can be treated independently and an input u_C can be rejected as implausible if it is implausible for *any* output. A more in-depth alternative for multiple outputs is also available (Vernon et al., 2010).

Defining inputs as “implausible” is straightforward. Starting with observation data,

$y_F(x)$, and mean surrogate predictions $\mu_N(x, u_C)$, u_C is implausible if, for any $y_F(x)$

$$\frac{|y_F(x) - \mu_N(x, u_C)|}{\sqrt{\sigma_N^2(x, u_C) + \sigma_{MD}^2(x) + \sigma_\epsilon^2(x)}} \geq 3. \quad (5.3)$$

Quantities σ_N^2 , σ_{MD}^2 , and σ_ϵ^2 are respectively: the variance of the surrogate, the model discrepancy, and the observational error. If, for a given u_C , the difference between an observation and the surrogate prediction is sufficiently big then u_C is declared implausible. The number 3 comes from Pukelsheim (1994) who shows that at least 95% of *any* unimodal distribution is contained within three standard deviations.

Specification of these variances is critical. While σ_N^2 is obtained from the surrogate, the choices for σ_{MD}^2 and σ_ϵ^2 are subjective. For example, Andrianakis et al. (2017) take $\sigma_\epsilon^2 + \sigma_{MD}^2$ as $\rho^2/4$, where ρ is the range of the observed output. Andrianakis et al. (2015) instead take σ_ϵ^2 as $\rho^2/4$ and σ_{MD}^2 as $0.1\sigma_N^2$. Boukouvalas et al. (2014b) elicit values of $\sigma_{MD}^2(x) = 0.15\mu_N(x, u_C)$ and $\sigma_\epsilon^2(x) = 0.02y_F(x)$. Choices for the variances can be lowered at later waves should the non-implausible set stay too large, decreasing the tolerance for an input to still be considered non-implausible. It is possible that no values of u_C are deemed non-implausible, which is the so-called terminal case (Salter et al., 2019). This usually means that σ_{MD}^2 is set too low or that the simulator is poor.

One advantage of HM is that only simple surrogates may be needed in early waves (Salter and Williamson, 2016), leading to computational savings and avoiding statistical complexities. Implementing HM often proceeds by discretizing the input space into a large set of candidate values for u_C . At each wave, new simulation runs (and a new surrogate fit) are used to rule-out more and more of these candidate values. When there are many waves, generating new candidate values at each wave can be necessary due to enormous shrinking of the non-implausible set. Andrianakis et al. (2017) provide one method for generating new, non-implausible, candidate values.

HM and KOH. With KOH, estimation of u_C is confounded with discrepancy, but predictions and their uncertainties are available. However, implementing KOH in complex problems may be burdensome if not intractable. Speculatively, a hybrid strategy may be to use HM to reduce the input space, confirm the absence of the terminal case, and then apply KOH in the narrowed space to get predictions and uncertainties. Complex models would be ones for which this approach would be most appealing; whereas the Fish and Ocean examples in this review have been intentionally simplified. Nonetheless, hybrid strategies remain a topic for further exploration.

5.3 Approximate Bayesian Computation (ABC)

Obtaining posterior distributions for calibration parameters u_C and predictions (the KOH approach in Section 5.1) can be computationally challenging. ABC methods offer an alternative to the full KOH approach. In moderately complex contexts they have been found useful (Rutter et al., 2018); but less so in more ambitious settings (McKinley et al., 2018).

In the simplest example, an ABC method aims to produce samples from $\pi(\theta|Y_F)$, the posterior distribution of unknowns θ given the field data Y_F . For calibration, think of θ as u_C . ABC does this by generating samples for the unknowns $\theta^{(s)}$ and the output $z^{(s)}$ from $\pi(Y_F|\theta)\pi(\theta)$, that is, from the likelihood of the data given the unknowns, multiplied by the prior probability of the unknowns. Such samples are only accepted if $z^{(s)} = Y_F$. For continuous settings, where exact equality cannot occur, acceptance is instead made if $B(z^{(s)}, Y_F) < \tau$ where B is a measure of distance and τ a level of tolerance. An approximated posterior distribution is then given by the collection of accepted $\theta^{(s)}$ s. The choice of τ is important - if τ is small then it may take a very long time to generate a single sample that satisfies the inequality, but if τ is not small then the approximation to the posterior is less reliable. This tradeoff between accuracy and computability is a problem. When there are multiple outputs (or there are other controllable inputs x , and thus for any given $\theta^{(s)}$, there are effectively multiple outputs), Y_F and $z^{(s)}$ can be replaced with informative summary statistics. How to choose a single statistic that sufficiently represents all of the outputs is challenging.

For stochastic computer models, simulating from the likelihood is equivalent to running the simulator (or from the surrogate). Following Wilkinson (2013), τ can be interpreted as a bound on the observational error and model discrepancy, leading to a “correct” posterior rather than an approximation. Similar to HM, choice of τ is partially subjective.

Efficiently searching for new θ s to accept (or reject) is not always clearcut and a variety of search methods have been suggested; see McKinley et al. (2018) for a summary. If ABC is done without the use of a surrogate, many runs of the simulator itself (one every time a new candidate for θ is tested) are needed. Otherwise, too few accepted θ will be generated or an overly high value of τ will be required. In either case accuracy can be compromised. With a surrogate, runs are cheap, removing an important computational barrier.

Fish Example. Applying ABC to the fish simulator in order to estimate how many fish are in the total population, assume that 25 fish captured in the first round are recaptured in the second round. A straightforward method to determine the total population size is to simulate many times from the simulator, for many different values of the total fish population, and “accept” a simulation every time it leads to 25 fish being recaptured. This is exactly ABC, and is a fairly common practice with agent-based models. Doing so 10,000 times, using a uniform prior on the integers between 200 and 4000, so each such population size has prior probability $1/3801$, yields the results in the left panel of Figure 7. This direct use of the simulator produces only 52 accepted samples from the 10,000 runs. In comparison, a hetGP surrogate fit from only 400 simulator runs, and from which 1,000,000 samples are quickly drawn, yields 3503 accepted samples. That result, illustrated in the right panel of Figure 7, gives a less noisy histogram with the same overall shape. If the agent-based model is even marginally costly the value of a surrogate in ABC computations is high.

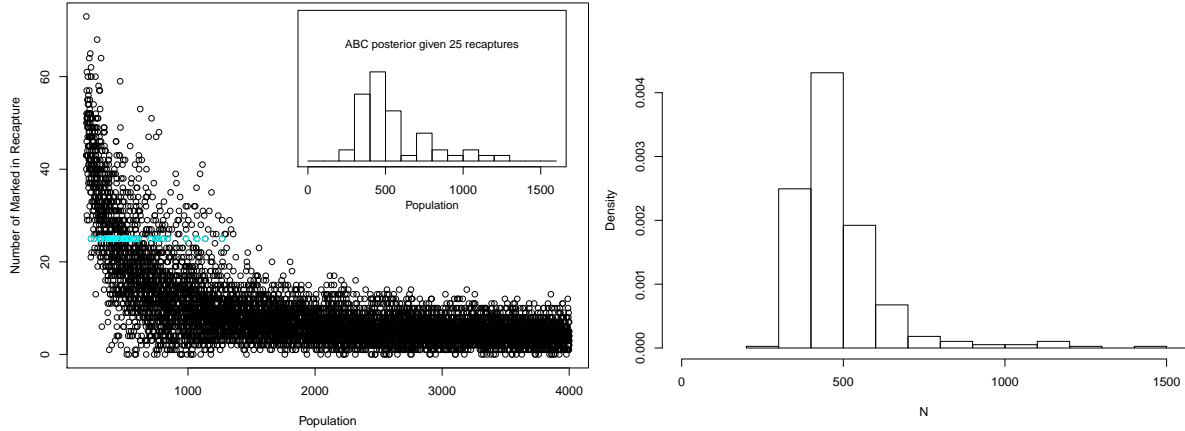


Figure 7: ABC calibration results for the fish simulator, using the simulator itself (left) and a hetGP surrogate (right). The prior distribution for the true population size is uniform on the integers in $[200, 4000]$, the observation (number of recaptured fish) is 25. The left plot shows 10,000 simulations, highlights the 52 in agreement with the observation, and the histogram of accepted simulations. The histogram in the right plot is for the 3503 accepted draws out of 1,000,000 from the hetGP surrogate.

5.4 Bound-to-Bound

The three calibration techniques above are the more popular techniques in the literature; but others also exist. A similar technique to HM, Bound-to-Bound (B2B), developed in the engineering literature, and compared to KOH by Frenklach et al. (2016), formulates the calibration problem as

$$y_F(x) = y_S(x, u_C) + E(x) \quad (5.4)$$

The surrogate y_S is typically a quadratic polynomial, but other functions can be accommodated. $E(x)$ is an error term bounded above and below and sweeps up all uncertainties. Quadratic programming then produces feasible values (bounds) for u_C , values such that the difference between field and simulator lie within the bounds for E .

5.5 Bayesian Melding

Another related technique is Bayesian Melding (Poole and Raftery, 2000; Raftery et al., 1995). The original motivating application combined expert judgement, historical data, and a population dynamics model to help manage the bowhead whale population and harvesting policies for the International Whaling Commission. A prior distribution, π_1 , was elicited for model outputs. Prior distributions were also elicited for model inputs, but these induced a different prior distribution, π_2 , for the outputs. Bayesian Melding makes use of logarithmic pooling to reconcile differences between π_1 and π_2 ($\pi = \pi_1^\alpha \pi_2^{(1-\alpha)}$) and produce an updated prior for the inputs. The resulting formalism

is essentially the same as that of Bayesian computer model calibration, though the two approaches emphasize different aspects of the same problem.

Since the original application, Bayesian Melding has been applied in applications that include ecology, epidemiology, urban modelling, and pollution monitoring (Ševčíková et al., 2007; Alkema et al., 2007; Radtke et al., 2002; Fuentes and Raftery, 2005). In most of these settings, the computational model is sufficiently fast so that parameter estimation and posterior sampling can be carried out directly, without a surrogate. In other settings, a single complex model run is used in the melding analysis. While the use of surrogates is compatible within the melding formulation, surrogates are far more common in Bayesian computer model calibration and History Matching settings where computationally demanding models with uncertain input parameters are more common.

6 Other Methods and Objectives

This section briefly outlines some other techniques for prediction and for other objectives.

6.1 Regression Trees

In some situations the simulator mean M may have discontinuities or “regime changes”, where a very different relationship between y and x exists in one part of input space compared to another part (i.e., non-stationarity). Regression Trees (Breiman et al., 1984) form a class of methods that can be useful in these situations. They are also useful in contexts where some inputs are categorical rather than numerical. The problems are treated by dividing the input space into mutually exclusive regions within which independent surrogates (GPs or other regression methods) are fit.

Two approaches, the TreedGP (TGP Gramacy and Lee, 2008) and Bayesian Additive Regression Trees (BART Chipman et al., 2010) have found wide use and application. Both use the data to automatically partition the input space, rely on Bayesian computation, and have software available: TreedGP in `tgp` on CRAN (Gramacy and Taddy, 2016; Gramacy, 2007); BART in several R packages, including `BayesTree` (Chipman and McCulloch, 2016) and `BART` (McCulloch et al., 2019). Specific details for categorical inputs in `tgp` are found in Broderick and Gramacy (2011) and Section 2 of Gramacy and Taddy (2010).

Other approaches by Rulli re et al. (2018), and by users of Voronoi tessellations instead of trees (e.g., Kim et al., 2005; Rushdi et al., 2017; Park and Apley, 2018), have received less attention. Pratola et al. (2017) extends BART to heteroscedastic σ_v^2 (HBART) by modeling M as a sum of Bayesian regression trees (as in BART) and the intrinsic variance $\sigma_v^2(x)$ as a product of Bayesian regression trees, in a joint approach similar to that in Section 3.2.

Calibration methods capitalizing on the KOH approach and using regression trees as in TGP (Section 6.1) are explored in Konomi et al. (2017). In each terminal node of the partition a GP with an independent constant intrinsic variance term is assumed for the computer model output. An independent GP is also deployed for the discrepancy term. Because the constant σ_v^2 can vary across terminal nodes, heteroscedasticity is automatic.

6.2 Qualitative Inputs

Categorical (qualitative) variables are often present in stochastic simulators, especially those that incorporate characteristics of human behavior. While regression trees (Section 6.1) are capable of dealing with categorical inputs, there are extensions of the GP methods that are also available and likely more effective for problems with smooth output.

Qian et al. (2008), Zhou et al. (2011), and Chen et al. (2013) describe ways to extend the correlation functions used for numerical inputs to incorporate qualitative variables. Painting with a broad brush, their approaches take the correlation between two outputs $y(x_i)$ and $y(x_j)$ as the product of two correlation functions: $C_c(w_i, w_j)$ dealing with the continuous inputs, w , and $C_q(z_i, z_j)$ for the qualitative variables, z . A simple way of building C_q takes

$$C_q(w_i, w_j) = \prod_{k=1}^K \tau_{k, w_{ik}, w_{jk}} \quad (6.1)$$

where K is the number of qualitative variables and $\tau_{k, w_{ik}, w_{jk}}$ represents the correlation between w_{ik} and w_{jk} . One example of $\tau_{k, w_{ik}, w_{jk}}$ is:

$$\tau_{j, w_{ik}, w_{jk}} = \exp\{-(\phi_{ik} + \phi_{jk})I[w_{ik} \neq w_{jk}]\} \quad (6.2)$$

where I is the indicator function ($= 1$ if its argument is true, $= 0$ if false), and $\phi > 0$. The references cited above also provide other ways of modeling $\tau_{k, w_{ik}, w_{jk}}$. Alternative methods exist for modeling qualitative inputs, including via latent variables Zhang et al. (2018).

6.3 Optimization

A common experimental objective is to maximize an output of the simulator, i.e., to find an input x_{\max} that maximizes the output $y(x)$. (If the objective is to minimize, replace $y(x)$ by $-y(x)$). An example: look for an intervention that best mitigates an epidemic. Finding an optimum is usually a sequential process where successive x s are chosen to get closer and closer to the optimal x_{\max} . After obtaining initial simulator runs ($y(x_1), \dots, y(x_N)$) and building a surrogate model, new runs can be chosen by maximizing an “acquisition function”, α : $x_{\text{new}} = \arg \max_x \alpha(x)$.

One such, the “probability of improvement” acquisition function $\alpha_{\text{PI}}(x) = \Pr(y(x) > y_{\max})$, where $y_{\max} = \max(y(x_1), \dots, y(x_N))$ is the current observed maximum, was proposed by Kushner (1964), though it may be inefficient when the objective function is multi-model (Jones, 2001). A widely accepted alternative is the *expected improvement* (EI) acquisition function (Mockus et al., 1978; Jones et al., 1998):

$$\alpha_{\text{EI}}(x) = E[\max(y(x) - y_{\max}, 0)]. \quad (6.3)$$

Maximizing EI chooses the input x_{new} that maximizes the expected increase in the maximum value of observed runs. If y is modeled by a GP

$$\alpha_{\text{EI}}(x) = (y_{\max} - \mu_N(x))\Phi\left(\frac{\mu_N(x) - y_{\max}}{\sigma_N(x)}\right) + \sigma_N(x)\phi\left(\frac{y_{\max} - \mu_N(x)}{\sigma_N(x)}\right) \quad (6.4)$$

where $\mu_N(x)$ is the predictive mean of the GP, $\sigma_N(x)$ the standard deviation, ϕ is the standard normal density, and Φ the standard normal distribution function. Successive iterations lead to a progressively improved estimate for the maximum. A recent review of Bayesian optimization methods can be found in Frazier (2018).

This formulation is sensible for deterministic simulators but for stochastic simulators, $y(x)$ is random, and so optima are less concretely defined — the output is different every time the simulator is run at the same x . Consequently, interest then lies in maximizing a quantity of interest, such as the mean M , or possibly another scalar quantity such as the q^{th} quantile. If said quantity is the mean M , then y_{\max} can be replaced with the maximum estimated mean of currently run inputs, $\mu_{\max} = \max_{i \in \{1, \dots, N\}} \mu_N(x_i)$, (Vazquez et al., 2008), or the maximum estimated mean of any possible input, $\max_x \mu_N(x)$ (Gramacy and Lee, 2011). Similar substitutions could be made for different quantities of interest. If the quantity of interest is modeled with a GP (as M is in Sections 3.1 and 3.2, and the q^{th} quantile is in Section 3.3.1), then Equation 6.4 can be applied.

Alternative criteria to EI, specifically designed for stochastic problems, also exist within the same framework. Jalali et al. (2016) provide a brief summary of some alternative criteria, as well as an in depth comparison between them. An R package for implementing several stochastic optimization methods (including some choices for the replacements of y_{\max}), using the homGP model from Section 3.1, is available in (`DiceOptim`; Picheny et al. (2016); Picheny and Ginsbourger (2014)). Section 4.2 of Binois and Gramacy (2018a) describes how `hetGP` methods can be combined with EI.

The related goal of level set estimation to find regions where the output exceeds a threshold T can be targeted with sequential criteria similar to EI. A simple criterion is maximum contour uncertainty (MCU), wherein new points are chosen to maximize the expected probability of misclassification, acquiring simulation runs close to the boundary between $y(x) < T$ and $y(x) > T$. Lyu et al. (2018) provide an example using a `hetGP` surrogate, and some discussion of related criteria. Also see Binois and Gramacy (2018a).

6.4 Sensitivity Analysis

Determining and measuring the effect of inputs on the output is usually part of any simulator experiment. Doing so assists scientific understanding of the system and enables screening out potentially superfluous variables. This goal has many related names: sensitivity analysis, screening, variable selection, etc., but the overall objective is generally the same - summarize and measure the influence of each input.

For deterministic simulators, Sobol indices (Sobol, 1993) are widely used. Probabilistic distributions are assumed on the inputs of the simulator in order to represent their range of variations. Then, a functional Analysis of Variance (ANOVA) decomposition splits the variation of the simulator output into multiple components, each representing the individual contribution of an input variable x_j or combination of input variables. A Sobol index is then computed as the percentage of the total simulator output variation explained by a component. Key Sobol indices include the main effects, the percentage of variation explained by the individual x_j s *alone*. The variation explained by the interactive additive effect between any set of input variables can also be computed. Computing the components takes large numbers of runs but the use of surrogate GPs make the calculations feasible (Schonlau and Welch, 2006; Marrel et al., 2009). An enveloping discussion of sensitivity is in Oakley and O’Hagan (2004).

Two extensions, by Marrel et al. (2012) and Hart et al. (2017), of the definition of Sobol indices for stochastic simulators yield the following expression for the stochastic simulator:

$$y(x) = y(x, \epsilon_{\text{seed}}) \quad (6.5)$$

where x is the set of controllable inputs while ϵ_{seed} is an input responsible for stochasticity in the output. The input ϵ_{seed} is a stand-in for the intrinsic variability, and can be called a seed variable. As with a deterministic simulator, a probabilistic distribution (typically uniform) is assumed to represent the range of variation in controllable inputs.

In Marrel et al. (2012), the total variation in the *mean* of the stochastic simulator is analysed through the functional ANOVA decomposition and Sobol indices are computed based on the percentage of the total *simulator* variation each component explains. The variation explained by the seed variable ϵ_{seed} can also be computed, representing the total variation explained by the intrinsic variance. Additionally, a sensitivity analysis of the intrinsic variance $\sigma_N^2(x)$ can be conducted separately to gather information on which input variables most impact the heteroscedasticity.

Hart et al. (2017) assumes the simulator can be run at different inputs x with the same seed ϵ_{seed} . Rather than building a joint stochastic simulator surrogate for the mean and variance, as described in Section 3.2, they build a separate surrogate for a number of seeds. For each seed, they obtain a realization of each Sobol index, and by aggregating the realizations, they obtain distributions for the indices.

The extensive literature on model selection may have counterparts that can be effective for stochastic simulators. But a fully satisfactory approach even for deterministic simulators remains somewhat elusive.

7 Concluding Remarks

Within this review there have been several key messages:

Gaussian Process Surrogates. It is rarely, if ever, the case that a full analysis of a problem can be run without some kind of statistical model. Emphasis on GP surrogates is driven by four considerations: it is a Bayesian method permitting defensible evaluation of uncertainties; it relies on the data to choose from exceptionally wide possibilities; it is computationally feasible when the number of parameters is moderate; it is widely applicable. For a given problem other types of surrogates might replace GPs but will likely lack a measure of universality. Alternatives or modifications to GPs are often necessary when input dimension is large, the number of unique inputs in the data is very large, or when outputs are discontinuous.

Design. It is commonly observed that the presence of randomness in a stochastic simulator demands much larger sample sizes than would be expected in the deterministic case. Moreover, replicates are an integral part of the design issue and generally treated in arbitrary ways. Several questions raised in Section 4 have no precursors in deterministic settings and form a suite of enticing and important targets for research. Rules of thumb, while imperfect, can be useful starting points for practitioners. For deterministic simulators Loeppky et al. (2009) recommend a total simulator budget of $N = 10d$, where d is the dimension of the inputs x . No such simple/well explored recommendations exist yet for stochastic simulators.

Calibration. There is no obvious one-size-fits-all method for calibrating a simulator, and a major reason for this is the presence of model discrepancy. A broad empirical comparison is needed with guidance about which strategies are effective under which conditions. Assessing the effectiveness of different methods can be challenging (see McKinley et al., 2018), involving a variety of statistical issues and computational barriers, while requiring the contexts of the application to be considered.

The Link with Deterministic Simulators. Almost all of the strategies documented and employed here have roots in the treatment of deterministic simulators. The presence of intrinsic variability, v , has led to non-trivial extensions such as hetGP, but also newer methods such as QK. There may be other tactics and methods in the deterministic literature that can be extended for use with stochastic simulators. Alternatively, some problems, whether those addressed within this review or otherwise, may require methodology that has no analogue within the deterministic literature.

These messages spawn some specific questions examples including:

- Are GPs needed for the intrinsic variance $\sigma_v^2(x)$, or is a parametric form, as in Boukouvalas et al. (2014a) good enough? If so, how can a parametric form be chosen?
- The extent to which intrinsic variability in stochastic simulators can safely be assumed Gaussian is unclear, though Normality of v is generally assumed throughout this review, except in Section 3.3. Are there other paths to pursue?

- A number of specific design questions are posed in Section 4 (e.g., number of replicates vs unique space filling points in a single stage design). The importance of sequential and multi-stage designs raises the question of how to spur their adoption in practice.
- Since stochastic simulators are under control of the modeler, it is possible to fix seeds that generate the intrinsic randomness. To what extent this can be used to treat specific problems is questionable, though in sensitivity analysis (see Section 6.4) it has played a role. Coupling stochastic simulators with deterministic simulators has also been explored (Baker et al., 2019).
- Complex stochastic simulators (say, with large numbers of uncertain inputs) may, in some instances, be replaced by a less complex one (e.g. Molina et al., 2005) that captures key features of the original simulator. This strategy is invariably application specific and an important question may be when, and how, to utilize the idea in contexts that would otherwise require infeasible numbers of runs.

This review strives to raise awareness of existing tools and strategies for treating stochastic simulators and provide a good starting point for practitioners interested in utilizing up-to-date statistical approaches. It is apparent that there is a general shortage of statistical research in this field. The problems are pervasive and challenging. They pose computational and technical questions, as well as theoretical and philosophical ones. Current solutions may often be capable, but there is a general lack of comprehensive comparison between different solutions, and a lack of testing of their generalizability to situations such as very large data sets. The hope is that the review provokes statistical researchers to engage the open questions discussed.

Acknowledgements

We gratefully acknowledge the support and funding provided by SAMSI during the Model Uncertainty: Mathematical and Statistical program, 2018-19. Moreover, Professor David Banks, Director of SAMSI, is thanked for suggesting and encouraging the writing of this review.

RBG gratefully acknowledged funding from a DOE LAB 17-1697 via subaward from Argonne National Laboratory for SciDAC/DOE Office of Science ASCR and High Energy Physics, and from National Science Foundation (NSF) award DMS-1821258.

Pierre Barbillon has received the support of the EU in the framework of the Marie-Curie FP7 COFUND People Programme, through the award of an Agree-Skills/AgreeSkills+ fellowship (under grant agreement n°609398).

References

- Abt, M. and Welch, W. J. (1998). Fisher information and maximum-likelihood estimation of covariance parameters in gaussian stochastic processes. *Canadian Journal of Statistics*, 26(1):127–137.
- Adigaa, A., Agashea, A., Arifuzzamana, S., Barretta, C. L., Beckmana, R., Bisseta, K., Chena, J., Chungbaeka, Y., Eubanka, S., Gupta, E., et al. (2015). Generating a synthetic population of the united states.
- Alkema, L., Raftery, A. E., Clark, S. J., et al. (2007). Probabilistic projections of hiv prevalence using bayesian melding. *The annals of applied statistics*, 1(1):229–248.
- Andrianakis, I., McCreesh, N., Vernon, I., McKinley, T. J., Oakley, J. E., Nsubuga, R. N., Goldstein, M., and White, R. G. (2017). Efficient history matching of a high dimensional individual-based HIV transmission model. *SIAM/ASA Journal on Uncertainty Quantification*, 5(1):694–719.
- Andrianakis, I., Vernon, I. R., McCreesh, N., McKinley, T. J., Oakley, J. E., Nsubuga, R. N., Goldstein, M., and White, R. G. (2015). Bayesian history matching of complex infectious disease models using emulation: a tutorial and a case study on HIV in Uganda. *PLoS computational biology*, 11(1):e1003968.
- Ankenman, B., Nelson, B. L., and Staum, J. (2010). Stochastic kriging for simulation metamodeling. *Operations research*, 58(2):371–382.
- Ba, S. (2019). *SLHD: Maximin-Distance (Sliced) Latin Hypercube Designs*. R package version 1.1.2.
- Ba, S., Joseph, V. R., et al. (2012). Composite gaussian process models for emulating expensive functions. *The Annals of Applied Statistics*, 6(4):1838–1860.
- Baker, E., Challenor, P., and Eames, M. (2019). Predicting the output from a stochastic computer model when a deterministic approximation is available. *arXiv preprint arXiv:1902.01290*.
- Bayarri, M., Berger, J., Cafeo, J., Garcia-Donato, G., Liu, F., Palomo, J., Parthasarathy, R., Paulo, R., Sacks, J., Walsh, D., et al. (2007a). Computer model validation with functional output. *The Annals of Statistics*, 35(5):1874–1906.
- Bayarri, M. J., Berger, J. O., Paulo, R., Sacks, J., Cafeo, J. A., Cavendish, J., Lin, C.-H., and Tu, J. (2007b). A framework for validation of computer models. *Technometrics*, 49(2):138–154.
- Begon, M. et al. (1979). *Investigating animal abundance: capture-recapture for biologists*. Edward Arnold (Publishers) Ltd.

- Binois, M. and Gramacy, R. (2018a). **hetGP**: Heteroskedastic Gaussian process modeling and sequential design in R. *available as a vignette in the R package*.
- Binois, M. and Gramacy, R. B. (2018b). *hetGP: Heteroskedastic Gaussian Process Modeling and Design under Replication*. R package version 1.1.1.
- Binois, M., Gramacy, R. B., and Ludkovski, M. (2018a). Practical heteroscedastic gaussian process modeling for large simulation experiments. *Journal of Computational and Graphical Statistics*, 0(0):1–14.
- Binois, M., Huang, J., Gramacy, R. B., and Ludkovski, M. (2018b). Replication or exploration? sequential design for stochastic simulation experiments. *Technometrics*, 0(0):1–17.
- Bisset, K. R., Chen, J., Feng, X., Kumar, V., and Marathe, M. V. (2009). Epifast: a fast algorithm for large scale realistic epidemic simulations on distributed memory systems. In *Proceedings of the 23rd international conference on Supercomputing*, pages 430–439. ACM.
- Boukouvalas, A. and Cornford, D. (2009). Learning heteroscedastic gaussian processes for complex datasets. Technical report, Aston University, Neural Computing Research Group.
- Boukouvalas, A., Cornford, D., and Stehlík, M. (2014a). Optimal design for correlated processes with input-dependent noise. *Computational Statistics & Data Analysis*, 71:1088–1102.
- Boukouvalas, A., Sykes, P., Cornford, D., and Maruri-Aguilar, H. (2014b). Bayesian precalibration of a large stochastic microsimulation model. *IEEE Transactions on Intelligent Transportation Systems*, 15(3):1337–1347.
- Breiman, L., Friedman, J., Olshen, R., and Stone, C. (1984). Classification and regression trees. monterey, ca: Wadsworth. wadsworth statistics/probability series.
- Broderick, T. and Gramacy, R. (2011). Classification and categorical inputs with treed Gaussian process models. *Journal of classification*, 28(2):244–270.
- Brynjarsdóttir, J. and O’Hagan, A. (2014). Learning about physical parameters: The importance of model discrepancy. *Inverse Problems*, 30(11):114007.
- Chen, H., Loepky, J. L., Sacks, J., Welch, W. J., et al. (2016). Analysis methods for computer experiments: how to assess and what counts? *Statistical science*, 31(1):40–60.
- Chen, X., Wang, K., and Yang, F. (2013). Stochastic kriging with qualitative factors. In *2013 Winter Simulations Conference (WSC)*, pages 790–801. IEEE.

- Chipman, H., George, E., and McCulloch, R. (2010). BART: Bayesian additive regression trees. *The Annals of Applied Statistics*, 4(1):266–298.
- Chipman, H. and McCulloch, R. (2016). *BayesTree: Bayesian Additive Regression Trees*. R package version 0.3-1.4.
- Chung, M., Binois, M., Gramacy, R. B., Bardsley, J. M., Moquin, D. J., Smith, A. P., and Smith, A. M. (2019). Parameter and uncertainty estimation for dynamical systems using surrogate stochastic processes. *SIAM Journal on Scientific Computing*, 41(4):A2212–A2238.
- Conti, S. and O’Hagan, A. (2010). Bayesian emulation of complex multi-output and dynamic computer models. *Journal of Statistical Planning and Inference*, 140(3):640 – 651.
- Craig, P. S., Goldstein, M., Seheult, A. H., and Smith, J. A. (1997). Pressure matching for hydrocarbon reservoirs: a case study in the use of bayes linear strategies for large computer experiments. In *Case studies in Bayesian statistics*, pages 37–93. Springer.
- Damblin, G., Barbillon, P., Keller, M., Pasanisi, A., and Parent, É. (2018). Adaptive numerical designs for the calibration of computer codes. *SIAM/ASA Journal on Uncertainty Quantification*, 6(1):151–179.
- Fadikar, A., Higdon, D., Chen, J., Lewis, B., Venkatramanan, S., and Marathe, M. (2018). Calibrating a stochastic, agent-based model using quantile-based emulation. *SIAM/ASA Journal on Uncertainty Quantification*, 6(4):1685–1706.
- Farah, M., Birrell, P., Conti, S., and Angelis, D. D. (2014). Bayesian emulation and calibration of a dynamic epidemic model for a/h1n1 influenza. *Journal of the American Statistical Association*, 109(508):1398–1411.
- Feynman, R. P. (1948). Space-time approach to non-relativistic quantum mechanics. *Rev. Mod. Phys.*, 20:367–387.
- Frazier, P. I. (2018). A tutorial on bayesian optimization. *arXiv preprint arXiv:1807.02811*.
- Frenklach, M., Packard, A., Garcia-Donato, G., Paulo, R., and Sacks, J. (2016). Comparison of statistical and deterministic frameworks of uncertainty quantification. *SIAM/ASA Journal on Uncertainty Quantification*, 4(1):875–901.
- Fricker, T. E., Oakley, J. E., and Urban, N. M. (2013). Multivariate gaussian process emulators with nonseparable covariance structures. *Technometrics*, 55(1):47–56.
- Fuentes, M. and Raftery, A. E. (2005). Model evaluation and spatial interpolation by bayesian combination of observations with outputs from numerical models. *Biometrics*, 61(1):36–45.

- Gneiting, T. and Raftery, A. E. (2007). Strictly proper scoring rules, prediction, and estimation. *Journal of the American Statistical Association*, 102(477):359–378.
- Goldberg, P. W., Williams, C. K., and Bishop, C. M. (1998). Regression with input-dependent noise: A gaussian process treatment. In *Advances in neural information processing systems*, pages 493–499.
- Gramacy, R. (2007). tgp: an R package for bayesian nonstationary, semiparametric nonlinear regression and design by treed gaussian process models. *Journal of Statistical Software*, 19(9):6.
- Gramacy, R. and Lee, H. (2008). Bayesian treed Gaussian process models with an application to computer modeling. *Journal of the American Statistical Association*, 103(483):1119–1130.
- Gramacy, R. and Taddy, M. (2010). Categorical inputs, sensitivity analysis, optimization and importance tempering with tgp version 2, an R package for treed Gaussian process models. *Journal of Statistical Software*, 33(6):1–48.
- Gramacy, R. B. and Lee, H. K. H. (2009). Adaptive design and analysis of supercomputer experiments. *Technometrics*, 51(2):130–145.
- Gramacy, R. B. and Lee, H. K. H. (2011). Optimization under unknown constraints. In Bernardo, J., Bayarri, S., Berger, J. O., Dawid, A. P., Heckerman, D., Smith, A. F. M., and West, M., editors, *Bayesian Statistics 9*, pages 229–256. Oxford University Press.
- Gramacy, R. B. and Taddy, M. A. (2016). *tgp: Bayesian Treed Gaussian Process Models*. R package version 2.4-14.
- Gu, M. and Wang, L. (2018). Scaled gaussian stochastic process for computer model calibration and prediction. *SIAM/ASA Journal on Uncertainty Quantification*, 6(4):1555–1583.
- Hart, J. L., Alexanderian, A., and Gremaud, P. A. (2017). Efficient computation of indices for stochastic models. *SIAM Journal on Scientific Computing*, 39(4):A1514–A1530.
- Harville, D. A. (1998). Matrix algebra from a statistician’s perspective.
- Henderson, D. A., Boys, R. J., Krishnan, K. J., Lawless, C., and Wilkinson, D. J. (2009). Bayesian emulation and calibration of a stochastic computer model of mitochondrial dna deletions in substantia nigra neurons. *Journal of the American Statistical Association*, 104(485):76–87.

- Herbei, R. and Berliner, L. M. (2014). Estimating ocean circulation: An mcmc approach with approximated likelihoods via the bernoulli factory. *Journal of the American Statistical Association*, 109(507):944–954.
- Higdon, D., Gattiker, J., Williams, B., and Rightley, M. (2008). Computer model calibration using high-dimensional output. *Journal of the American Statistical Association*, 103(482):570–583.
- Jalali, H., Van Nieuwenhuyse, I., and Picheny, V. (2016). Comparison of kriging-based methods for simulation optimization with heterogeneous noise. *European Journal of Operational Research*.
- Jolliffe, I. (2011). *Principal component analysis*. Springer.
- Jones, D., Schonlau, M., and Welch, W. (1998). Efficient global optimization of expensive black-box functions. *Journal of Global Optimization*, 13(4):455–492.
- Jones, D. R. (2001). A taxonomy of global optimization methods based on response surfaces. *Journal of global optimization*, 21(4):345–383.
- Kac, M. (1949). On distributions of certain wiener functionals. *Transactions of the American Mathematical Society*, 65:1–13.
- Kennedy, M. C. and O’Hagan, A. (2001). Bayesian calibration of computer models. *Journal of the Royal Statistical Society: Series B (Statistical Methodology)*, 63(3):425–464.
- Kersaudy, P., Sudret, B., Varsier, N., Picon, O., and Wiart, J. (2015). A new surrogate modeling technique combining kriging and polynomial chaos expansions—application to uncertainty analysis in computational dosimetry. *Journal of Computational Physics*, 286:103–117.
- Kersting, K., Plagemann, C., Pfaff, P., and Burgard, W. (2007). Most likely heteroscedastic gaussian process regression. In *Proceedings of the 24th International Conference on Machine Learning*, pages 393–400.
- Kim, H., Mallick, B., and Holmes, C. (2005). Analyzing nonstationary spatial data using piecewise Gaussian processes. *Journal of the American Statistical Association*, 100(470):653–668.
- Kleijnen, J. P. (2009). Kriging metamodeling in simulation: A review. *European journal of operational research*, 192(3):707–716.
- Kleijnen, J. P. (2017). Regression and kriging metamodels with their experimental designs in simulation: a review. *European Journal of Operational Research*, 256(1):1–16.

- Koenker, R. and Bassett Jr, G. (1978). Regression quantiles. *Econometrica: journal of the Econometric Society*, pages 33–50.
- Konomi, B., Karagiannis, G., Lai, K., and Lin, G. (2017). Bayesian treed calibration: an application to carbon capture with AX sorbent. *Journal of the American Statistical Association*, 112(517):37–53.
- Kushner, H. J. (1964). A new method of locating the maximum point of an arbitrary multipeak curve in the presence of noise. *Journal of Basic Engineering*, 86(1):97–106.
- Lee, A. (2015). *pyDOE: The experimental design package for python*. Python package version 0.3.8.
- Liu, F., Bayarri, M., Berger, J., et al. (2009). Modularization in bayesian analysis, with emphasis on analysis of computer models. *Bayesian Analysis*, 4(1):119–150.
- Loeppky, J. L., Sacks, J., and Welch, W. J. (2009). Choosing the Sample Size of a Computer Experiment - A Practical Guide. *Technometrics*, 51(4):366–376.
- Lyu, X., Binois, M., and Ludkovski, M. (2018). Evaluating gaussian process meta-models and sequential designs for noisy level set estimation. *arXiv preprint arXiv:1807.06712*.
- Marrel, A., Iooss, B., Da Veiga, S., and Ribatet, M. (2012). Global sensitivity analysis of stochastic computer models with joint metamodels. *Statistics and Computing*, 22(3):833–847.
- Marrel, A., Iooss, B., Laurent, B., and Roustant, O. (2009). Calculations of sobol indices for the gaussian process metamodel. *Reliability Engineering & System Safety*, 94(3):742–751.
- McCulloch, R., Sparapani, R., Gramacy, R., Spanbauer, C., and Pratola, M. (2019). *BART: Bayesian Additive Regression Trees*. R package version 2.7.
- McKay, M. D., Beckman, R. J., and Conover, W. J. (1979). Comparison of three methods for selecting values of input variables in the analysis of output from a computer code. *Technometrics*, 21(2):239–245.
- McKeague, I. W., Nicholls, G., Speer, K., and Herbei, R. (2005). Statistical inversion of south atlantic circulation in an abyssal neutral density layer. *Journal of Marine Research*, 63(4):683–704.
- McKinley, T. J., Vernon, I., Andrianakis, I., McCreesh, N., Oakley, J. E., Nsubuga, R. N., Goldstein, M., White, R. G., et al. (2018). Approximate bayesian computation and simulation-based inference for complex stochastic epidemic models. *Statistical science*, 33(1):4–18.

- Mockus, J., Tiesis, V., and Zilinskas, A. (1978). The application of Bayesian methods for seeking the extremum. *Towards Global Optimization*, 2(117-129):2.
- Molina, G., Bayarri, M. J., and Berger, J. O. (2005). Statistical inverse analysis for a network microsimulator. *Technometrics*, 47(4):388–398.
- Moutoussamy, V., Nanty, S., and Pauwels, B. (2015). Emulators for stochastic simulation codes. *ESAIM: Proceedings and Surveys*, 48:116–155.
- Oakley, J. E. and O’Hagan, A. (2004). Probabilistic sensitivity analysis of complex models: a bayesian approach. *Journal of the Royal Statistical Society: Series B (Statistical Methodology)*, 66(3):751–769.
- Oakley, J. E. and Youngman, B. D. (2017). Calibration of stochastic computer simulators using likelihood emulation. *Technometrics*, 59(1):80–92.
- O’Hagan, A. (2006). Bayesian analysis of computer code outputs: A tutorial. *Reliability Engineering and System Safety*, 91(10-11):1290–1300.
- Park, C. and Apley, D. (2018). Patchwork kriging for large-scale gaussian process regression. *The Journal of Machine Learning Research*, 19(1):269–311.
- Paulo, R., García-Donato, G., and Palomo, J. (2012). Calibration of computer models with multivariate output. *Computational Statistics & Data Analysis*, 56(12):3959–3974.
- Pedregosa, F., Varoquaux, G., Gramfort, A., Michel, V., Thirion, B., Grisel, O., Blondel, M., Prettenhofer, P., Weiss, R., Dubourg, V., Vanderplas, J., Passos, A., Cournapeau, D., Brucher, M., Perrot, M., and Duchesnay, E. (2011). Scikit-learn: Machine learning in Python. *Journal of Machine Learning Research*, 12:2825–2830.
- Picheny, V. and Ginsbourger, D. (2014). Noisy kriging-based optimization methods: a unified implementation within the diceoptim package. *Computational Statistics & Data Analysis*, 71:1035–1053.
- Picheny, V., Ginsbourger, D., and Roustant, O. (2016). *DiceOptim: Kriging-Based Optimization for Computer Experiments*. R package version 2.0.
- Plumlee, M. (2017). Bayesian calibration of inexact computer models. *Journal of the American Statistical Association*, 112(519):1274–1285.
- Plumlee, M. and Tuo, R. (2014). Building accurate emulators for stochastic simulations via quantile kriging. *Technometrics*, 56(4):466–473.
- Poole, D. and Raftery, A. E. (2000). Inference for deterministic simulation models: the bayesian melding approach. *Journal of the American Statistical Association*, 95(452):1244–1255.

- Pratola, M., Chipman, H., George, E., and McCulloch, R. (2017). Heteroscedastic bart using multiplicative regression trees. *arXiv preprint arXiv:1709.07542*.
- Pronzato, L. and Müller, W. G. (2011). Design of computer experiments: space filling and beyond. *Statistics and Computing*, 22(3):681–701.
- Pukelsheim, F. (1994). The three sigma rule. *The American Statistician*, 48(2):88–91.
- Qian, P. Z. G., Wu, H., and Wu, C. J. (2008). Gaussian process models for computer experiments with qualitative and quantitative factors. *Technometrics*, 50(3):383–396.
- Radtke, P. J., Burk, T. E., and Bolstad, P. V. (2002). Bayesian melding of a forest ecosystem model with correlated inputs. *Forest Science*, 48(4):701–711.
- Raftery, A. E., Givens, G. H., and Zeh, J. E. (1995). Inference from a deterministic population dynamics model for bowhead whales. *Journal of the American Statistical Association*, 90(430):402–416.
- Rasmussen, C. E. and Williams, C. K. (2006). *Gaussian Processes for Machine Learning*, volume 2. MIT press Cambridge, MA.
- Reynolds, C. W. (1987). Flocks, herds and schools: A distributed behavioral model. In *Proceedings of the 14th annual conference on Computer graphics and interactive techniques*, pages 25–34.
- Roustant, O., Ginsbourger, D., and Deville, Y. (2018). **DiceKriging: Kriging Methods for Computer Experiments**. R package version 1.5.6.
- Rulli re, D., Durrande, N., Bachoc, F., and Chevalier, C. (2018). Nested kriging predictions for datasets with a large number of observations. *Statistics and Computing*, 28(4):849–867.
- Rushdi, A., Swiler, L., Phipps, E., D’Elia, M., and Ebeida, M. (2017). VPS: Voronoi piecewise surrogate models for high-dimensional data fitting. *International Journal for Uncertainty Quantification*, 7(1).
- Rutter, C., Ozik, J., DeYoreo, M., and Collier, N. (2018). Microsimulation model calibration using incremental mixture approximate bayesian computation. *arXiv preprint arXiv:1804.02090*.
- Sacks, J., Welch, W. J., Mitchell, T. J., and Wynn, H. P. (1989). Design and analysis of computer experiments. *Statistical science*, pages 409–423.
- Salter, J. M. and Williamson, D. (2016). A comparison of statistical emulation methodologies for multi-wave calibration of environmental models. *Environmetrics*, 27(8):507–523.

- Salter, J. M., Williamson, D. B., Scinocca, J., and Kharin, V. (2019). Uncertainty quantification for computer models with spatial output using calibration-optimal bases. *Journal of the American Statistical Association*, 0(0):1–24.
- Santner, T. J., B., W., and W., N. (2018). *The Design and Analysis of Computer Experiments, Second Edition*. Springer-Verlag.
- Schonlau, M. and Welch, W. J. (2006). Screening the input variables to a computer model via analysis of variance and visualization. In *Screening*, pages 308–327. Springer.
- Ševčíková, H., Raftery, A. E., and Waddell, P. A. (2007). Assessing uncertainty in urban simulations using bayesian melding. *Transportation Research Part B: Methodological*, 41(6):652–669.
- Shah, A., Wilson, A., and Ghahramani, Z. (2014). Student-t processes as alternatives to gaussian processes. In *Artificial intelligence and statistics*, pages 877–885.
- Sobol, I. M. (1967). On the distribution of points in a cube and the approximate evaluation of integrals. *Computational Mathematics and Mathematical Physics*, 7(4):86–112.
- Sobol, I. M. (1993). Sensitivity estimates for nonlinear mathematical models. *Mathematical modelling and computational experiments*, 1(4):407–414.
- Spiller, E. T., Bayarri, M., Berger, J. O., Calder, E. S., Patra, A. K., Pitman, E. B., and Wolpert, R. L. (2014). Automating emulator construction for geophysical hazard maps. *SIAM/ASA Journal on Uncertainty Quantification*, 2(1):126–152.
- Stein, M. L. (2012). *Interpolation of spatial data: some theory for kriging*. Springer Science & Business Media.
- Sullivan, T. J. (2015). *Introduction to uncertainty quantification*, volume 63. Springer.
- Sun, F., Gramacy, R., Haaland, B., Lu, S., and Hwang, Y. (2019). Synthesizing simulation and field data of solar irradiance. *Statistical Analysis and Data Mining*, 12(4):311–324. Preprint on arXiv:1806.05131.
- Tuo, R. and Wu, C. (2016). A theoretical framework for calibration in computer models: parametrization, estimation and convergence properties. *SIAM/ASA Journal on Uncertainty Quantification*, 4(1):767–795.
- Tuo, R., Wu, C. J., et al. (2015). Efficient calibration for imperfect computer models. *The Annals of Statistics*, 43(6):2331–2352.
- Vazquez, E., Villemonteix, J., Sidorkiewicz, M., and Walter, E. (2008). Global optimization based on noisy evaluations: an empirical study of two statistical approaches. In *Journal of Physics: Conference Series*, volume 135, page 012100. IOP Publishing.

- Vernon, I., Goldstein, M., Bower, R. G., et al. (2010). Galaxy formation: a bayesian uncertainty analysis. *Bayesian Analysis*, 5(4):619–669.
- Wang, W. and Haaland, B. (2018). Controlling sources of inaccuracy in stochastic kriging. *Technometrics*, pages 1–13.
- Wang, Z., Shi, J. Q., and Lee, Y. (2017). Extended t-process regression models. *Journal of Statistical Planning and Inference*, 189:38–60.
- Wilensky, U. (1999). NetLogo. <http://ccl.northwestern.edu/netlogo/>. *Center for Connected Learning and ComputerBased Modeling Northwestern University Evanston IL*.
- Wilkinson, R. D. (2013). Approximate bayesian computation (abc) gives exact results under the assumption of model error. *Statistical applications in genetics and molecular biology*, 12(2):129–141.
- Xie, G. and Chen, X. (2017). A heteroscedastic t-process simulation metamodeling approach and its application in inventory control and optimization. In *Simulation Conference (WSC), 2017 Winter*, pages 3242–3253. IEEE.
- Yohan Chalabi, Christophe Dutang, P. S. and Wuertz, D. (2019). *randtoolbox: Toolbox for Pseudo and Quasi Random Number Generation and Random Generator Tests*. R package version 1.30.0.
- Zhang, B., Cole, D., and Gramacy, R. (2020). Distance-distributed design for Gaussian process surrogates. *To appear in Technometrics*. Preprint on arXiv:1812.02794.
- Zhang, Q. and Xie, W. (2017). Asymmetric kriging emulator for stochastic simulation. In *Proceedings of the 2017 Winter Simulation Conference*, page 137. IEEE Press.
- Zhang, Y., Tao, S., Chen, W., and Apley, D. W. (2018). A latent variable approach to gaussian process modeling with qualitative and quantitative factors. *arXiv preprint arXiv:1806.07504*.
- Zhou, Q., Qian, P. Z., and Zhou, S. (2011). A simple approach to emulation for computer models with qualitative and quantitative factors. *Technometrics*, 53(3):266–273.